Published in final edited form as:
J Comp Neurol. 2011 June 15; 519(9): 1797–1815. doi:10.1002/cne.22602.

N-cadherin regulates primary motor axons growth and branching during zebrafish embryonic development

Juan L Brusés[1]
Department of Anatomy and Cell Biology, University of Kansas School of Medicine, Kansas City, KS 661610

Abstract

N-cadherin is a classical type I cadherin that contributes to the formation of neural circuits by regulating growth cone migration and the formation of synaptic contacts. This study analyzed the role of N-cadherin in primary motor axons growth during development of the zebrafish (*Danio rerio*) embryo. After exiting the spinal cord, primary motor axons migrate ventrally through a common pathway and form the first neuromuscular junction with the muscle pioneer cells located at the horizontal myoseptum, which serves as a choice point for cell-type specific pathway selection. Analysis of N-cadherin mutants (*cdh2*^{hi3644Tg}) and embryos injected with N-cadherin antisense morpholinos showed primary motor axons extending aberrant axonal branches at the choice point in ~40% of the somitic hemisegments, and an ~150% increase in the number of branches per axon length within the ventral myotome. Analysis of individual axons trajectories showed that the caudal (CaP) and rostral (RoP) motor neurons axons formed aberrant branches at the choice point which abnormally extended in the rostrocaudal axis and ventrally to the horizontal myoseptum. Expression of a dominant-interfering N-cadherin cytoplasmic domain in primary motor neurons caused some axons to abnormally stall at the horizontal myoseptum and to impair their migration into the ventral myotome. However, in N-cadherin depleted embryos the majority of primary motor axons innervated their appropriate myotomal territories indicating that N-cadherin regulates motor axon growth and branching without severely affecting the mechanisms that control axonal target selection.

Keywords

Cell adhesion molecules; N-cadherin; zebrafish development; primary motor neurons; axonal pathfinding; neuromuscular junction

Introduction

Cell adhesion molecules of the cadherin superfamily mediate calcium-dependent homotypic binding between apposed cell membranes, as well as cell autonomous regulation of cell behavior (Takeichi, 1991; Zhu and Luo, 2004). Cadherins participate in various tissue morphogenetic processes during development and tissue repair, by regulating the dynamics of the interactions between cellular surfaces (Gumbiner, 2005). In the nervous system, different cadherins are expressed in distinct regions of the neural tube during particular developmental periods, and regulate the formation of boundaries between neural tube segments, the migration of neurons within and outside the neural tube, and the formation of neuronal connections (Katsamba et al., 2009; Price et al., 2002; Redies and Takeichi, 1996;

[1]Corresponding author: University of Kansas School of Medicine, Department of Anatomy and Cell Biology, 3901 Rainbow Blvd, MS 3038, Kansas City, KS 66160, jbruses@kumc.edu, Phone: 913-588-1790, Fax: 913-588-2710.

Takeichi, 2007; Tepass et al., 2000). N-cadherin is a classical type I cadherin widely expressed in the nervous system (Hatta et al., 1987), which has been implicated in the establishment of neural circuits by regulating growth cone migration and the formation of synaptic contacts (Bozdagi et al., 2004; Kadowaki et al., 2007; Riehl et al., 1996). When presented as a purified protein substrate or when expressed on the surface of heterologous cell lines, N-cadherin promotes neurite outgrowth (Bixby and Zhang, 1990; Matsunaga et al., 1988; Payne et al., 1992). This N-cadherin activity is blocked by the addition of function-blocking antibodies (Neugebauer et al., 1988), suggesting that N-cadherin provides a permissive substrate for axonal growth. Furthermore, expression of dominant-interfering N-cadherin cytoplasmic domains lacking the entire extracellular domain (ΔED), affects the growth of retinal ganglion cells axons *in vivo* (Riehl et al., 1996). However, expression of ΔED N-cadherin cytoplasmic domain in cultured hippocampal neurons results in abnormal elongation of dendritic spines (Togashi et al., 2002), indicating that disruption of N-cadherin activity can promote or inhibit neurite growth depending on the cell type and cellular environment.

This evidence supports the view that N-cadherin mediated cell-cell interactions regulate axonal growth, as well as the stabilization of intercellular contacts required for the development of synaptic connections. Axonal migration towards a specific destination is commonly assisted by intermediate targets or choice points in which transient interactions between the growth cone and a specialized group of cells influence axonal behavior (Goodman and Shatz, 1993). A variety of cell surface molecules involved in the interactions between the growth cone and the cells at the choice point have been identified including semaphorins and receptor tyrosine phosphatases (Desai et al., 1996; Krueger et al., 1996; Winberg et al., 1998; Yu et al., 1998). In addition, regulation of cell adhesion appears to be a mechanism that can directly influence axonal growth at intermediate targets. For example *beaten path*, a secreted immunoglobulin superfamily protein, regulates the adhesive properties of Fasciclin II and contributes to motor axon pathway selection in *Drosophila* through a mechanism that resembles the regulation of cell adhesion by polysialylated neural cell adhesion molecule (NCAM) in vertebrate motor neurons (Fambrough and Goodman, 1996; Holmes and Heilig, 1999; Tang et al., 1992). This suggests that cell adhesion molecules may regulate motor axon growth at sites of transient interactions between the growth cone and the cells that constitute a choice point.

In the zebrafish (*Danio rerio*) embryo, each somitic hemisegment is first innervated by three primary motor neurons named as rostral (RoP), middle (MiP), and caudal (CaP). Primary motor axons exit the neural tube and migrate ventrally through a common pathway adjacent to the notochord until reaching the horizontal myoseptum (Eisen et al., 1986; Eisen et al., 1990; Myers et al., 1986; Westerfield et al., 1986). At this point, the axons establish the first neuromuscular junction with the muscle pioneer cells before proceeding to innervate cell-type specific myotomal territories (Melancon et al., 1997). Spinal cord motor neurons and muscle pioneer cells, both express N-cadherin mRNA at the time motor axons reach the horizontal myoseptum (Cortes et al., 2003), suggesting that N-cadherin may contribute to axonal pathway selection at the choice point. Zebrafish embryos in which N-cadherin expression is suppressed by mutations in the N-cadherin gene (*cdh2*) or by injection of N-cadherin antisense morpholinos, showed normal development of muscle pioneer cells, although defective migration of a subpopulation of adaxial muscle cells was detected in some somitic segments (Birely et al., 2005; Cortes et al., 2003). However, defective motor axon growth has been observed in N-cadherin mutant embryos (Birely et al., 2005; Lele et al., 2002), suggesting that N-cadherin participates in motor axon migration during innervation of the myotome. Thus, the present study was aimed at analyzing whether N-cadherin contributes to the regulation of primary motor axon outgrowth and cell-type

specific pathway selection during innervation of the myotomal territories in the zebrafish embryo.

Materials and Methods

Fish strains, breeding, and generation of transgenic lines

Zebrafish were obtained from the Zebrafish International Resource Center (ZIRC, Eugene, OR), raised and maintained as described in The Zebrafish Book (Westerfield, 2000), and staged as previously reported (Kimmel et al., 1995). The zebrafish AB line was used as wild type strain (strain AB-3, stock # 5560). In addition, this study used the N-cadherin mutant *cdh2*$^{hi3644Tg/+}$ (AB/TU) (stock # 2795) fish line (Amsterdam et al., 1999; Amsterdam et al., 2004) (here called *cdh2*^{hi3644Tg}), and the transgenic line *Tg(mnx1:GFP)ml2*/+ AB (ZIRC catalog ID ZL1163)(previously known as *Tg(hlxb9:GFP)ml2)*, which expresses green fluorescent protein (GFP) under the *mnx1* promoter (also known as *hb9, hlxb9, scra1, and hoxhb9*) (Flanagan-Steet et al., 2005). To generate a stable transgenic fish expressing the yeast Gal4 transcriptional activator (Brand and Perrimon, 1993; Davison et al., 2007) fused to a virally derived VP16 activator sequence (Gal4-VP16) in motor neurons (*Tg(mnx1:Gal4-VP16)*), a plasmid was generated carrying the *mnx1* promoter (a gift from D. Meyer from the University of Freiburg) followed by the Gal4-VP16 sequence (Koster and Fraser, 2001), a SV40 polyadenylation (pA) signal, and flanked by the Tol2 transposable elements (Kawakami et al., 1998) (Fig 1 A). This plasmid was constructed in the Tol2 plasmid system developed by K. Kawakami and C-B. Chien using bacterial recombination (Gateway, Invitrogen, Carlsbad, CA)(Kwan et al., 2007; Suster et al., 2009). The plasmid was injected together with *in vitro* transcribed transposase mRNA into 1-cell stage wild type embryos. Messenger RNA was synthesized using the mMESSAGE mMachine kit (Ambion, Austin TX). Embryos were raised to adulthood, mated with wild type animals, and DNA from F1 eggs was extracted using the DNeasy kit (Qiagen, Valencia, CA) and used as template for a polymerase chain reaction (PCR) amplification using primers annealing to the Gal4 sequence (Forward, 5' ATGAAGCTACTGTCTTCTATCG; and Reverse, 5' TGTCTTTGACCTTTGTTACTA C) to identify animals with germ-line transmission. Offspring from the *Tg(mnx1:Gal4-VP16)* F0 carriers were injected at the 1-cell stage with a plasmid encoding prenylated enhanced GFP (pren-EGFP) driven by a 14X-upstream activation sequence (UAS) fused to the fish basal promoter *E1b* derived from the carp β-actin (14X-UAS) (Koster and Fraser, 2001; Scheer and Campos-Ortega, 1999) and examined at 24 hours post fertilization (hpf) for EGFP expression in motor neurons. Plasmid injections were carried out with an air-pressured Picospritzer III microinjector (Parker, Cleveland, OH) using glass microneedles. Plasmid DNA was prepared using endotoxin free plasmid kits (Qiagen) and diluted in injection solution (0.2M KCl, 0.04% phenol red) at a final concentration of 50 ng/μL, and 1–2 nL were injected into the cell of 1-cell stage embryos. The use and manipulation of animals used in this study has been approved by the Institutional Animal Care and Use Committee from the University of Kansas School of Medicine.

Antibody and α-bungarotoxin labeling

Embryos were dechorionated, anesthetized and sacrificed in ice-cold E3 embryo medium (NaCl, 5mM; KCl, 0.17mM; CaCl2, 0.33 mM; and MgSO4, 0.33mM) containing 0.4% tricaine (MS222, Ethyl 3-aminobenzoate methanesulfonate salt, Sigma-Aldrich, St Louis, MO), immersed in ice-cold 4% paraformaldehyde (Electron Microscopy Sciences, Hatfield, PA) containing 1% dimethyl sulfoxide (DMSO) in phosphate buffer saline, pH 7.4 (PBS), fixed for 3 h at room temperature (RT) followed by 10 min incubation in methanol at −20°C, washed in PBS, and incubated in blocking solution (2% bovine serum albumin (BSA) in PBS) for 1 h at RT. One hundred and twenty hpf embryos were treated with collagenase

(1 mg/ml)(Worthington Biomedical Corp., Lakewood, NJ) for 10 min at 37°C before incubation in blocking solution (2% BSA, 0.5% Triton X-100, in PBS). Embryos were then incubated in blocking solution containing primary antibodies overnight at 4°C, washed in PBS, incubated with corresponding secondary antibodies conjugated with Cy3 (Jackson ImmunoResearch, West Grove, PA) washed, deyolked, and mounted in Prolong Gold (Invitrogen). For labeling of nicotinic acetylcholine receptors, α-bungarotoxin (α-BTX) Alexa 488 conjugated (Molecular Probes, Eugene, OR) (final concentration 10 μg/ml) was added to the antibody solution.

Antibody characterization

The following primary antibodies were used (Table 1):

Znp1, mouse monoclonal IgG anti-zebrafish synaptotagmin 2 (Developmental Studies Hybridoma Bank (DSHB), Iowa City, IA) detected a single band of ~60 kDa in immunoblots from zebrafish homogenates, and from mouse cerebellum and synaptosomes homogenates (Fox and Sanes, 2007; Trevarrow et al., 1990). Zebrafish embryos immunostained with znp1 antibodies showed the same distribution and localization in motor axons as was previously reported (Jiang et al., 1996).

SV2, mouse monoclonal IgG anti-elasmobranch synaptic vesicle protein 2 (SV2, DSHB) detected a single band of ~100 kDa in immunoblots from synaptosome and membrane brain fractions from various species (Buckley and Kelly, 1985). SV2 immunostaining of zebrafish embryos and larvae showed the same pattern of cellular morphology and distribution in motor axons as was reported in previous studies (Panzer et al., 2005)

Rabbit polyclonal IgG anti-zebrafish N-cadherin (a gift from Q. Liu from the University of Akron) detected a single band of ~120 kDa, which is the expected size for zebrafish N-cadherin, in immunoblot from zebrafish brain extracts (Liu et al., 2001). A single band of ~120 kDa (between the 105 kDa and 160 kDa molecular weight marker) was detected in Western blots from zebrafish tissue extracts in the present study (Fig 2 A).

MNCD2, rat monoclonal IgG anti-mouse N-cadherin detected a single band of ~116 kDa in immunoblots from mouse fetal brain homogenates (Matsunami and Takeichi, 1995) (MNCD2, DSHB). A single band of ~120 kDa (between the 105 kDa and 160 kDa molecular weight markers), which corresponds to the expected size for zebrafish N-cadherin, was detected in Western blots from zebrafish homogenates (Fig 2 A). The molecular weight of the band detected by MNCD2 coincides with the molecular weight of the band detected by the rabbit polyclonal IgG anti zebrafish N-cadherin. The protein detected by MNCD2 was substantially decreased in immunoblots from N-cadherin mutant zebrafish embryos (*cdh2*^{hi3644Tg}) and from embryos treated with N-cadherin antisense morpholinos (Fig 3 H, I). MNCD2 also labeled Chinese Hamster Ovary cells transfected with zebrafish N-cadherin while no labeling was detected in untransfected cells (Fig 2 B1 – B4). Whole mount immunostaining of 24 hpf zebrafish embryos with MNCD2 antibodies (Fig 2 C – F) revealed the same pattern of protein expression as was previously reported for N-cadherin mRNA (Cortes et al., 2003).

36/E-cadherin, mouse monoclonal anti-human E-cadherin (BD Transduction Laboratories, 610181) detected a single band of ~120 kDa in immunoblots from A431 cells lysate (Akins et al., 2007) and detected two bands of ~120 kDa and 140 kDa (between the 105 kDa and 160 kDa markers) in Western blots from zebrafish homogenates (Fig 3 J).

MHCD2500, mouse monoclonal IgG anti-human interleukin-2α subunit (IL2α) receptor (also known as CD25 or Tac)(Caltag, Burlingame, CA, MHCD2500, clone CD25-3G10).

MHCD2500 detected a single band of ~55 kDa in immunoblots from affinity purified human IL2α receptor (Leonard et al., 1984; Stockinger et al., 1990). The ability of the MHCD2500 antibody to recognize only IL2α receptor fusion proteins was determined by transfecting Human Embryonic Kidney 293 with a plasmid expressing the IL2α receptor C-terminally fused to EGFP (IL2α-EGFP) and immunolabeled with MHCD2500 followed by anti-mouse IgG Cy3 conjugated secondary antibody. Antibody staining co-localized with EGFP fluorescence while untransfected cells were not immunostained (data not shown). In addition, immunostaining of zebrafish embryos with MHCD2500 antibodies did not label cells or structures except for the cells transfected with the IL2α receptor fusion protein (Fig 8).

Cell culture and lipofection

Chinese Hamster Ovary (CHO) cells were grown in Ham's F12K medium (Gibco, Invitrogen) containing, 2 mM L-glutamine, 1.5 g/l sodium bicarbonate and 10 % fetal bovine serum (FBS), and plated in glass coversilp. CHO cell cultures were transfected using Lipofectamine 2000 (Invitrogen) following manufacturer's recommendations with a mix of two plamsids, one plasmid encoding Gal4-VP16 dowstream of a CMV promoter, and a second plasmid encoding zebrafish N-cadherin (a gift from J. Jontes) (AF418595) (Jontes et al., 2004) and pren-EGFP (each one under a 14X-UAS element), or encoding pren-EGFP under a 14X-UAS element. Forty-eight hours after transfection, CHO cells were fixed in 4% paraformaldehyde in PBS for 20 min at RT, blocked in PBS containing 2% BSA and 0.2% Triton-X100, incubated with MNCD2 antibodies for 2 h at RT in blocking solution, washed in PBS, incubated with anti-rat IgG Cy3 conjugated secondary antibodies for 2 h at RT in blocking solution, washed in PBS, and mounted in Prolong Gold mounting medium (Invitrogen). Human Embryonic Kidney 293 cells, were grown in MEM with Earl’s Salts (Gibco, Invitrogen) containing, 2 mM GlutaMAX (Invitrogen) , 0.1 mM Non-essential amino acids, 1.0 mM sodium pyruvate, 1.5 g/L sodium bicarbonate, and 10% FBS and lipofected as described above.

Image acquisition and analysis

Embryos were observed with a Nikon C1Si confocal microscope (Nikon, Tokyo, Japan) mounted on a Nikon Eclipse 90i upright microscope using a Plan-Apo 10X/0.45NA dry lens, and a Plan-Fluor 40X/NA1.3, a Plan-Apo 60X/NA1.4, and an Apo-TIRF 100X/NA1.49 oil immersion lenses. Samples were scanned at 1-μm intervals and stacks of confocal images were rendered to a single plane using EZ-C1 software (Nikon). Images were coded and randomly sorted so that the experimental condition was hidden to the investigator during image analysis. The images were analyzed using MetaMorph software (Universal Imaging Corporation, Downingtown, PA). Axon length was measured from the exit of the spinal cord as determined by the boundary of SV2 and znp1 labeling, up to the center of the axonal dilation formed at the horizontal myoseptum, and from this point up to the distal tip of the axon. Branches were measured from the center of the axon shaft to the tip of the protrusion and needed to be more than 3 μm long to be considered a branch. To determine presynaptic surface area, images from SV2 and znp1 immunostaining were threshold, distances calibrated, and a 10 μm × 10 μm square region was placed over the choice point region at the horizontal myoseptum, and the area of pixels with an intensity value above the threshold was measured an expressed in μm^2. Images were manipulated in Adobe Photoshop (Adobe Systems Incorporated, San Jose, CA) and changes in brightness and contrast were applied to the entire image.

Protein expression in motor neurons

Primary motor neurons were labeled by mosaic expression of pren-EGFP. Embryos were injected at the 1-cell stage with a mix of two plamsids, one plasmid encoding Gal4-VP16

dowstream of the *mnx1* promoter (Flanagan-Steet et al., 2005) and followed by a SV40 pA signal, and a second plasmid encoding pren-EGFP under a 14X-UAS fused *E1b* (Koster and Fraser, 2001; Scheer and Campos-Ortega, 1999) also followed by a SV40 pA signal. These plasmids were constructed in the Tol2 plasmid system (Kwan et al., 2007; Suster et al., 2009). To perturb N-cadherin in motor neurons, the zebrafish N-cadherin cytoplasmic domain (CD) (Lys 734 to Asp 893) was PCR amplified from the zebrafish N-cadherin cDNA and fused to the C-terminus of transmembrane portion of the IL2α human receptor subunit. The IL2α receptor subunit has no signaling or binding properties and can be immuno-labeled to detect the localization of the transfected protein (Katz et al., 1998). A bicistronic plasmid was generated containing the sequence of IL2α-N-cadherin-CD and pren-EGFP each one driven by a 14X-UAS element. As control, EGFP was fused to the C-terminus of IL2α. These plasmids were injected together with transposase mRNA into 1-cell stage *Tg(mnx1:Gal4-VP16)* embryos (Fig 1 B).

Morpholino injections

Morpholino (MO) oligonucleotides were purchased from Gene Tools (Philomath, OR) using previously reported sequences (Lele et al., 2002; von der Hardt et al., 2007). Antisense, cdh2-MO-UTR: 5'UTR″ (5'-TCTGTATAAAGAAACCGATAGAGTT-3'), corresponding to -40 to -16 N-cadherin mRNA sequence. Four bases mismatched, cdh2-MIS-MO: 5'-TCTCTATAAACAAACGGATAGTGTT-3'. Morpholinos were dissolved in water to a stock solution of 1 mM. For embryo injections the stock solution was diluted in injection solution to a final concentration of 50 μM and 1–2 nL injected into 1–2 cell stage embryos.

Western blot

Embryos were sacrificed in ice cold E3 medium containing 0.4% tricaine and homogenized by sonication in 150 μl of ice-cold extraction buffer (25 mM HEPES pH 7.2, 0.15M NaCl, 1% NP-40, EDTA-free protease inhibitors cocktail (Roche, Basel, Switzerland)) and cleared by centrifugation at 14,000 rpm for 20 min at 4°C. Protein content was determined by BCA assay (Pierce, Rockford, IL). Forty micrograms of total protein were diluted in 2X Laemmli sample buffer (Laemmli, 1970) and electrophoresed in a 10% sodium dodecyl sulfate (SDS) polyacrylamide gel, electro-transferred to polyvinylidene fluoride (PVDF) membranes (Immobilon-P, Amersham Biosciences, GE Healthcare, Piscataway, NJ), blocked in 3% non-fat dry milk (BioRad, Hercules, CA) solution in Tris-buffer saline, pH 7.6, with 1% Tween-20 (TBS-T), incubated in primary antibody, washed in TBS-T, and incubated with corresponding horseradish peroxidase-conjugated secondary antibodies diluted in TBS-T (Jackson ImmunoResearch, West Grove, PA). Secondary antibodies were detected by chemiluminescence (ECL) (Amersham Biosciences), the exposed film was digitized in a flat scanner, and the relative amount of protein was determined by densitometric analysis using the Gel Analysis tool of ImageJ software and measuring the area under the peaks.

Genotyping of cdh2^{hi3644Tg} mutants

Embryos were genotyped by PCR as previously described (Amsterdam et al., 1999). Briefly, a single embryo or the embryo's head was lysed in 50 μl of ELVIS lysis buffer (50 mM KCl, 10 mM Tris 8.5pH, 0.01% gelatin, 0.45% NP-40, 0.45% Tween-20, 5 mM EDTA, 200 μg/ml proteinase K), incubated for 2 h at 55°C followed by 15 min at 96°C. One microliter of the lysate was used as template for a PCR reaction (94°C for 2 min, 1 cycle; 94°C for 30 sec, 60°C for 30 sec, 72°C for 60 sec, 35 cycles; 72°C for 5 min, 1 cycle). Primers: ZN-CAD-1S (5' AACACGTCCTCAGAGTGCCAC) and ZN-CAD-2AS (5' GTACGGTTACCAAGTCAATGTG) which anneal to *cdh2*, and NLTR3 061127D (5' CTGTTCCATCTGTTCCTGAC) that anneals to the viral sequence. PCR products were separated by electrophoresis in 1.5% agarose gels, DNA stained with ethidium bromide, and observed in a UV transilluminator.

Electron microscopy

Embryos and larvae were fixed in 2.5% glutaraldehyde (Electron Microscopy Sciences, Hatfield, PA) and 1% DMSO in 0.1M cacodylic buffer pH 7.4 for 3 h at RT and overnight at 4°C, washed in PBS and postfixed in 1% osmium in 0.1M cacodylic buffer pH 7.4 for 1 h, rinsed in distilled water, progressively dehydrated in ethanol, and embedded in epoxy resin (EMBED 812, Electron Microscopy Sciences). Samples were sectioned at ~100 nm with a Leica UCT Ultramicrotome (Leica, Wetzlar, Germany), stained with 1% uranyl acetate for 35 min and with 1% lead citrate for 3 min, and observed and photographed with a JOEL 100CXII Transmission Electron Microscope (JOEL USA, Peabody, MA).

Results

N-cadherin is expressed by primary motor neurons and adaxial muscle pioneer cells

In the zebrafish embryo, N-cadherin mRNA is expressed throughout the developing somites and its expression is progressively down-regulated from rostral to caudal somites as myogenesis begins. By 20 hpf, N-cadherin mRNA is detected in all brain regions, eyes, neural tube, and adaxial slow muscle cells (Bitzur et al., 1994; Cortes et al., 2003; Liu et al., 2001; Warga and Kane, 2007). At this time, the myotomal fast muscle cells switch from expressing N-cadherin to express M-cadherin (Cortes et al., 2003). Adaxial muscle cells located dorsally and ventrally to the horizontal myoseptum, migrate radially from the notochord, and maintain N-cadherin expression while M-cadherin is up-regulated (Cortes et al., 2003). In contrast, muscle pioneer cells located at the level of the horizontal myoseptum do not migrate and maintain N-cadherin expression exclusively (Cortes et al., 2003; Devoto et al., 1996; Felsenfeld et al., 1991). To identify antibodies that recognize zebrafish N-cadherin, the cross-reactivity of commercially available antibodies raised against N-cadherin was first determined by Western blot analysis using zebrafish homogenates. A rabbit polyclonal antibody raised against zebrafish N-cadherin extracellular domain (provided by Dr Q. Liu)(Liu et al., 2001) identified a single band of ~120 kDa (between the 105 kDa and 160 kDa molecular weight marker) and was used as control (Fig 2 A, lane 1). The rat monoclonal MNCD2 antibody anti-mouse N-cadherin extracellular domain (Matsunami and Takeichi, 1995) detected a single band of ~120 kDa, which is the expected size for zebrafish N-cadherin (Fig 2 A, lane 2), suggesting that MNCD2 cross-reacts with zebrafish N-cadherin. To determine whether MNCD2 identifies zebrafish N-cadherin by immunostaining, CHO cells were transfected with a plasmid encoding zebrafish N-cadherin and pren-EGFP or with a plasmid expressing only pren-EGFP, fixed, incubated with MNCD2 antibodies followed by incubation with an anti-rat IgG Cy3-conjugated secondary antibody, and observed under confocal microscopy. Cells transfected with zebrafish N-cadherin showed a distinct labeling on the cell surface (Fig 2 B1, B2), while no signal was detected from cells expressing pren-EGFP alone (Fig 2 B3, B4), indicating that the MNCD2 antibody recognizes zebrafish N-cadherin.

To examine the expression pattern of N-cadherin at the protein level, 24 hpf wild type and *Tg(mnx1:GFP)ml2* zebrafish embryos were fixed and immunostained with anti-N-cadherin MNCD2 antibodies. *Tg(mnx1:GFP)ml2* zebrafish express GFP under the homeobox 1 gene *mnx1* promoter, and labels motor neurons soon after their last round of cell division (Flanagan-Steet et al., 2005). N-cadherin is expressed on the cell surface of neurons throughout the spinal cord including the soma of primary motor neurons (Fig 2 C, D). In addition, N-cadherin is detected on muscle pioneer fibers located at the horizontal myoseptum where primary motor axons form neuromuscular junctions as indicated by the clustering of acetylcholine receptors labeled with α-bungarotoxin (Fig 2 E and F). Thus, the pattern of expression of N-cadherin determined by immunolabeling matched the previously reported mRNA expression pattern (Cortes et al., 2003), indicating that N-cadherin is

expressed by both, primary motor neurons and muscle pioneer cells, at the time motor axons reach the horizontal myoseptum.

Analysis of the ultrastructure of neuromuscular junctions formed in the vicinity of the horizontal myoseptum in 24 hpf wild type zebrafish embryos revealed presynaptic terminals with the appearance of immature synaptic contacts having few synaptic vesicles and undifferentiated pre and postsynaptic densities (Fig 2 G). In addition, pre and postsynaptic membranes appeared in close apposition with each other, suggesting that the muscle basal lamina usually present at the synaptic cleft of neuromuscular junctions is still poorly differentiated at this developmental stage. In contrast, neuromuscular junctions in 120 hpf zebrafish larvae showed pre and postsynaptic membranes separated by a distinct electron dense material, which represents a specialized basal lamina (Sanes and Lichtman, 1999) (Fig 2 H). The basal lamina of mature synaptic contacts expands the distance between synaptic membranes and is believed to preclude direct protein interactions across the synaptic cleft. Thus, the pattern of N-cadherin expression and the ultrastructural features of neuromuscular junctions formed between primary motor axons and muscle pioneer cells at 24 hpf suggest that N-cadherin may engage in homophilic binding between pre and postsynaptic membranes.

Defective motor axon growth in N-cadherin depleted zebrafish embryos

To examine the role of N-cadherin in motor neuron development, motor axon morphology was analyzed in N-cadherin mutant zebrafish *cdh2*^{hi3644Tg} (Amsterdam et al., 2004), and in embryos injected with N-cadherin antisense morpholinos that knockdown N-cadherin expression (Lele et al., 2002; von der Hardt et al., 2007). The zebrafish mutant line *cdh2*^{hi3644Tg} was generated by retroviral insertional mutagenesis (Amsterdam and Hopkins, 1999) in which the viral insertion was mapped to the second intron of the N-cadherin gene (*cdh2*). This viral insertion results in a phenotype similar to the N-cadherin mutant *parachute (cdh2*$^{fr7/fr7}$), in which N-cadherin expression is lost, and is characterized by the disruption of the midbrain/hindbrain boundary and defective tail morphogenesis (Lele et al., 2002), suggesting that the viral insertion substantially impairs N-cadherin expression (Fig 3). Homozygotes *cdh2*^{hi3644Tg} mutants were obtained by crossing heterozygote *cdh2*^{hi3644Tg} adult animals. Mutant embryos were identified at 22–24 hpf by defective midbrain/hindbrain boundary formation (Fig 3 B – E), and their homozygocity for the viral insertion was determined by genotyping using PCR with a combination of primers flanking the viral insertion site, and primers that anneal to the viral sequence (Fig 3 G). The viral insertion appears to follow Mendelian inheritance in that ~25% of embryos from each cross were homozygotes (wild type = 27.5% ± 5.2, heterozygote = 44.4 ± 5.3, homozygote 28.1 ± 2.4 from 290 embryos obtained from five crosses). Furthermore, 97.7% of phenotypic mutant embryos were homozygote for the viral insertion and the remaining 2.3% were found to be heterozygote, indicating that the phenotype observed is associated with the viral insertion in *cdh2*.

The effect of the viral insertion on N-cadherin expression was examined by Western blot analysis using MNCD2 antibodies. Zebrafish embryos (24 hpf) from a cross between *cdh2*^{hi3644Tg} heterozygotes were genotyped and pooled as homozygotes (−;/−;), heterozygote (−;/+), and wild type (+/+). Two bands of ~105 kDa and ~120 kDa were detected in the immunoblot in wild type, heterozygote, and homozygote homogenates (Fig 3 H). The amount of protein was substantially reduced in *cdh2*^{hi3644Tg} homozygotes homogenates (Fig 3 H). The appearance of two bands instead of one ~120 kDa band detected in samples from 72 hpf wild type embryos (Fig 2 A) was probably due to changes of posttranslational modifications or to partial protein cleavage. N-cadherin was undetectable in an immunoblot of lysates from 120 hpf homozygote *cdh2*^{hi3644Tg} mutants (data not shown), indicating that the viral insertion substantially impairs N-cadherin

expression resulting in a *cdh2* hypomorph. Injection of antisense morpholinos targeted to the 5' UTR of N-cadherin mRNA (cdh2-MO-UTR) into 1-cell stage wild type embryos resulted in a similar phenotype observed in the *cdh2*^{hi3644Tg} mutants (Fig 3 C, F)(Lele et al., 2002). Immunoblot analysis of morpholino treated embryos using MNCD2 antibodies detected two bands of ~105 kDa and ~120 kDa (Fig 3 I). Treatment with antisense morpholino resulted in an almost complete elimination of N-cadherin expression as compared to embryos injected with a mismatched morpholino (Fig 3 I). Western blot analysis of morpholino injected embryos homogenates with an anti-E-cadherin antibody detected two bands of ~120 kDa and ~140 kDa. The amount of E-cadherin expression was not affected by the injection with antisense morpholinos targeted to the 5' UTR of N-cadherin mRNA (Fig 3 J).

Each somitic hemisegment in the zebrafish embryo is innervated by the RoP, MiP, and CaP primary motor neurons, and by ~25 secondary motor neurons that invade the myotome later in development (after 26 hpf)(Eisen et al., 1986; Myers et al., 1986; Westerfield et al., 1986). Cell division of primary motor neurons ends at ~16 hpf (Myers et al., 1986). The CaP motor axon is the first to exit the spinal cord at 19–20 hpf, and soon after, it is followed by the RoP and MiP axons (Myers et al., 1986). The three primary motor axons migrate through the common pathway delimited by the notochord (medially) and the myotome (laterally), and upon arrival to a choice point at the horizontal myoseptum, the growth cones make contact with the muscle pioneer cells and choose among three different cell-type specific pathways (Eisen et al., 1986; Melancon et al., 1997). While the CaP motor axon continues to migrate ventrally and innervates the ventral myotome, the MiP axon stops at the horizontal myoseptum and extends a branch that migrates dorsally to innervate the dorsal myotome. The RoP axon stops and form branches at the horizontal myoseptum to innervate muscle fibers in the vicinity of the myoseptum (Eisen et al., 1986; Melancon et al., 1997; Westerfield et al., 1986).

To examine whether N-cadherin contributes to axonal growth and pathfinding decision, *cdh2*^{hi3644Tg} mutants and N-cadherin antisense morpholino injected wild type embryos (cdh2-MO-UTR) were fixed at 24 hpf and immunostained with SV2 and znp1 antibodies which label all motor axons (Birely et al., 2005; Panzer et al., 2005). Embryos were examined by confocal microscopy and images obtained at the level of the yolk extension. In wild type and mismatched morpholino (cdh2-MO-MIS) injected embryos 100% of somitic hemisegments showed axons exiting the neural tube and extending ventrally through the common pathway up to the choice point, where a distinct axonal dilation is observed in the area of contact with the muscle pioneer cells (Fig 4 A – D)(Table 2). Similarly, in *cdh2*^{hi3644Tg} and cdh2-MO-UTR injected embryos, primary motor axons exited the spinal cord and migrated through the common pathway to the horizontal myoseptum. However, at the choice point and ventral to the horizontal myoseptum, axons extended aberrant branches within the myotome (Fig 4 E – H, Table 2). A ~150% increase in the number of branches per axon length and a ~45% increase in the average length of each branch were detected (Fig 4 I, J). A notable phenotype observed in *cdh2*^{hi3644Tg} motor axons was the extension of a prominent branch at the choice point (Fig 4 H). The average presynaptic surface area of the choice point neuromuscular junction was increased (~10%) in *cdh2*^{hi3644Tg} mutants and cdh2-MO-UTR treated embryos; however, the difference between groups was not statistically significant (Fig 4 K). This analysis indicates that the majority of primary motor axons outgrowth and migration through the common pathway up to the choice point was not affected by depletion of N-cadherin expression; however, axonal growth was disrupted at the horizontal myoseptum resulting in the formation of a higher number of axon branches.

After selecting cell-type specific pathways, primary motor axons invade their respective myotomal territories while forming *en-passant* synaptic contacts with muscle fibers (Panzer et al., 2005). Similarly to the primary motor neurons, secondary motor axons migrate into

different myotomal territories and branch to develop synaptic contacts. (Flanagan-Steet et al., 2005; Liu and Westerfield, 1992; Panzer et al., 2005; Panzer et al., 2006). To determine whether the increase in motor axon branching observed in 24 hpf *cdh2*^{hi3644Tg} mutants embryos leads to aberrant muscle innervation, wild type and *cdh2*^{hi3644Tg} mutants embryos were fixed at 120 hpf and labeled with SV2 antibodies and

Alexa 488 conjugated α-bungarotoxin to identify pre and postsynaptic components respectively. Embryos were observed under confocal microscopy, optical sections scanned at 1-μm interval over the ventral muscle, and stacks of ~30 μm were rendered to a single plane. In wild type embryos, neuromuscular junctions appeared evenly distributed throughout the muscle, formed the characteristic line of neuromuscular junctions at the somitic myosepta, and clusters of SV2 co-localized with postsynaptic α-bungarotoxin (Fig 5 A – C, G). In contrast, the density of pre and postsynaptic components was substantially increased in *cdh2*^{hi3644Tg} mutant embryos, and the distinct line of somitic myoseptal neuromuscular junctions observed in wild type animals became diffused due to the increase in axonal terminal arborization and in the number of neuromuscular junctions formed (Fig 5 D – E, H). To determine the density of neuromuscular junctions per surface area and the size of pre and postsynaptic components, 3-μm thick stacks from the central region of the ventral myotome in the medial-lateral axis were used to quantify SV2 and α-bungarotoxin clusters. This analysis showed a 58% and 45% increase in the number of SV2 and α-bungarotoxin clusters per 1000 μm^2 in *cdh2*^{hi3644Tg} mutant embryos as compared to age matched wild type embryos (Fig 5 I). In contrast, the average SV2 and α-bungarotoxin cluster size, and the degree of apposition between the two markers were not significantly affected in *cdh2*^{hi3644Tg} mutant embryos (Fig 5 J, K). This analysis indicates that the increase in axonal branching observed at 24 hpf leads to the formation of a higher number of neuromuscular junctions.

N-cadherin regulates CaP and RoP motor axon trajectories

To determine whether N-cadherin differently regulates motor axon growth in each of the primary motor neurons, individual axonal trajectories were examined. After making contact with the muscle pioneers cells at the horizontal myoseptum, the MiP motor axons extend a branch that migrate dorsally, which by 27 hpf has invaded the dorsal myotome. To examine MiP motor axons trajectories, wild type and *cdh2*^{hi3644Tg} mutant embryos were fixed at 27 hpf and immunostained with znp1 antibodies (Zhang and Granato, 2000). In all somitic hemisegments examined in both wild type and *cdh2*^{hi3644Tg} mutant embryos, a dorsal axon projection was observed, suggesting that MiP pathway selection was not disrupted in N-cadherin mutant embryos (Fig 6 A, B). However, while 97% of znp1 labeled dorsal motor axons in wild type embryos have a wild type phenotype, 70% of dorsal axons in *cdh2*^{hi3644Tg} mutant embryos were considered wild type (Table 3). The remaining 30% of dorsal axons did not follow a straight trajectory while growing into the dorsal myotome, but rather they appear to have followed a distorted zigzagged pattern of migration (Fig 6 B). To observe axonal trajectories of individual MiP neurons, motor neurons were labeled by mosaic expression of membrane-bound pren-EGFP. This was achieved by co-injecting a mix of two plasmids into 1-cell stage wild type and *cdh2*^{hi3644Tg} mutant embryos, one plasmid expressing Gal4-VP16 under the *mnx1* promoter, and a second plasmid expressing pren-EGFP under a 14X-UAS element. Embryos were fixed at 24 hpf and observed under confocal microscopy. All MiP labeled neurons in both *cdh2*^{hi3644Tg} mutant and wild type embryos showed the characteristic MiP axonal trajectory to the horizontal myoseptum and a dorsal axonal extension (Fig 6 C, D), indicating that MiP target selection is not affected in N-cadherin mutant embryos.

Mosaic expression of pren-EGFP was also used to examine CaP and RoP motor axon trajectories in wild type and *cdh2*^{hi3644Tg} mutant embryos. CaP and RoP motor neurons

were identified by their location in the spinal cord and axonal trajectories (Myers et al., 1986). In wild type and homozygote *cdh2*^{hi3644Tg} embryos, CaP axons migrated through the common pathway to the horizontal myoseptum and continued their ventral migration into the myotome (Fig 7 A – D). However, in 27% of cells analyzed in homozygote *cdh2*^{hi3644Tg} embryos, motor axons formed aberrant branches at the horizontal myoseptum in the rostrocaudal axis (Fig 7 C, D, Table 4). In addition, 91% of the labeled axons showed a defective phenotype as determined by their branching pattern at the choice point and/or ventral to the horizontal myoseptum (Table 4). Analysis of individually labeled RoP motor neurons in wild type embryos revealed their typical rostrocaudal trajectory through the spinal cord and ventrally into the somite until reaching the horizontal myoseptum (Myers et al., 1986). Similarly to wild type, RoP motor neurons in *cdh2*^{hi3644Tg} mutant embryos followed their stereotypic trajectory toward the horizontal myoseptum; however, in 33% of the cases the RoP axons formed aberrant branching at the horizontal myoseptum and in 22% of the cases the axons migrated into the ventral myotome (Fig 7 E – H, Table 4). This analysis shows that while the RoP and CaP axons migrated through the common pathway to the horizontal myoseptum, in some cases the motor axons extended aberrant branches at the choice point and invaded the ventral myotome.

N-cadherin dominant-interfering cytoplasmic domain affects CaP motor axon growth at the choice point

N-cadherin cytoplasmic domain binds to a variety of cytosolic proteins including the catenins which regulate cadherins function and contribute to the anchorage of cadherins to the actin cytoskeleton (Gumbiner, 2005). Expression of N-cadherin cytoplasmic domain lacking the entire ectodomain (ΔED) interferes with cadherin-mediated adhesion and affects axon growth, dendritic spine morphogenesis, and synapse formation (Riehl et al., 1996; Togashi et al., 2002). To examine cell autonomous effects of N-cadherin on motor axon behavior, N-cadherin cytoplasmic domain was fused to the C-terminus of the transmembrane domain of the IL2α subunit human receptor (Katz et al., 1998), and expressed in CaP motor neurons. To this end, a stable transgenic fish was generated expressing the yeast Gal4 transcriptional activator fused to a virally derived VP16 activator sequence (Gal4-VP16) under the *mnx1* promoter (*Tg(mnx1:Gal4-VP16)*). This promoter is active in postmitotic motor neurons (Arber et al., 1999; Tanabe et al., 1998), which in the zebrafish occurs at ~16 hpf (Myers et al., 1986). Therefore, expression of the exogenous protein cannot interfere with cell fate determination. Embryos obtained from animals with germ line transmission and injected at the 1-cell stage with a plasmid expressing pren-EGFP under a 14X-UAS showed mosaic EGFP expression in primary motor neurons at 24 hpf (Fig 8 A – D). To induce expression of the dominant-interfering N-cadherin cytoplasmic domain in primary motor neurons, *Tg(mnx1:Gal4-VP16)* embryos were injected at the 1-cell-stage with a bicistronic plasmid driving expression of N-cadherin cytoplasmic domain fused to IL2α (IL2α-cdh2-CD) under a 14X-UAS and pren-EGFP under a second 14X-UAS element to label the cell surface (Fig 7 A, F). Expression of the IL2α-cdh2-CD was confirmed by immunolabeling with anti-IL2α antibodies (Fig 8 G, H). As control, embryos were injected with a plasmid expressing the IL2α subunit C-terminally fused to EGFP (IL2α-EGFP), which was found evenly distributed over the entire cells surface (Fig 8 E, F). Similar to IL2α-EGFP, expression of IL2α-cdh2-CD was detected in the cell body and transported up to the distal end of the axon; however, IL2α-cdh2-CD localization was highly punctuated and accumulated at presumptive sites of cell-cell contacts including the horizontal myoseptum (Fig 8 G – I).

To examine cell autonomous roles of N-cadherin, embryos expressing IL2α-cdh2-CD and pren-EGFP, or IL2α-EGFP in CaP motor neurons were fixed at 24 hpf, immunostained with SV2 and znp1, and observed under confocal microscopy. Expression of IL2α-EGFP did not

affect CaP motor axons growth in that 100% of labeled motor axons reached the horizontal myoseptum at the same time as the untransfected neighboring cells, and showed normal axonal morphology. In addition, none of the IL2α-EGFP expressing CaP cells stalled at the horizontal myoseptum, indicating that expression of the foreign protein did not perturb motor axon growth (Fig 9 A–C, Table 5). Similarly to IL2α-EGFP expressing cells, 100% of CaP axons expressing IL2α-cdh2-CD exited the spinal cord and reached the horizontal myoseptum. However, expression of IL2α-cdh2-CD caused 26% of the CaP axons to abnormally stall at the horizontal myoseptum. In addition, 26% of CaP axons that extended ventrally to the myoseptum showed aberrant axonal morphology (Fig 9 D – I, Table 5). These results indicate that expression of a membrane bound ΔED N-cadherin cytoplasmic domain did not severely interfere with motor axon outgrowth and migration. However, IL2α-cdh2-CD expression disrupted motor axon growth at the choice point and its growth into the ventral myotome, indicating that perturbation of N-cadherin function only in the motor neuron was sufficient to affect motor axon behavior at the horizontal myoseptum.

Discussion

To evaluate the role of N-cadherin on primary motor axons growth and pathway selection two types of perturbations were used in this study namely, depletion of N-cadherin expression in the whole embryo, and mosaic expression of ΔED N-cadherin cytoplasmic domain in single motor neurons. Under both conditions, the majority of primary motor axons exited the spinal cord and migrated through the common pathway to the horizontal myoseptum, indicating that suppression of N-cadherin expression or interfering with cadherin function did not substantially affect axonal migration along the common pathway. However, depletion of N-cadherin in all tissues caused axons to grow aberrant branches, while expression of ΔED N-cadherin cytoplasmic domain in primary motor neurons caused some axons to stall at the horizontal myoseptum.

Previous analysis of N-cadherin mutant zebrafish embryos *cdh2*$^{fr7/fr7}$ (Lele et al., 2002) and *cdh2*^{p79emcf} (Birely et al., 2005) showed defective motor axons growth and abnormal axonal branching. Defective motor axon migration was not secondary to abnormal muscle development because the defects were still observed in somitic segments in which adaxial cells normally migrated (Birely et al., 2005). In some cases, motor axons were found to ectopically exit the spinal cord forming more than one ventral root, indicating that N-cadherin plays an earlier role in motor axon growth presumably a the point of exit from the spinal cord (Birely et al., 2005; Lele et al., 2002). In *cdh2*^{hi3644Tg} mutants used in the present study, similar axonal defects were occasionally observed before the axons reached the horizontal myoseptum. However, in the majority of the embryos examined axonal defects were found at the horizontal myoseptum, and therefore, this study focused on the analysis of this later event in axonal growth. Whether the frequency and type of axonal defects differs between different N-cadherin zebrafish mutants has not been determined.

In wild type embryos, CaP axons extend short branches at the choice point which are later retracted, indicating that the environment in the region of the muscle pioneer cells is permissive for the extension of axonal protrusions. However, the environment in the vicinity of the choice point also prevents those branches to stabilize and invade the myotome (Eisen et al., 1986; Liu and Westerfield, 1990; Myers et al., 1986; Westerfield et al., 1986). Depletion of N-cadherin expression caused aberrant growth of CaP motor axons, which extended branches at the choice point and ventral to the horizontal myoseptum that became stable and grew into the myotome. In addition, some RoP motor neurons, which normally stop and branch at the horizontal myoseptum, extended branches into the ventral myotome. However, the ability of the motor axons to reach their specific targets was not substantially impaired, in that the three primary motor axons innervated their corresponding myotomal

territories. This evidence indicates that the mechanisms that regulate axonal pathway selection at the choice point are not severely compromised in the absence of N-cadherin. However, the mechanisms that regulate the extension and retraction of axonal branches appear to be affected by the loss of N-cadherin expression, which in some cases may lead to the extension of axonal branches into inappropriate myotomal territories.

Aberrant axonal growth at the choice point has also been observed after laser ablation of muscle pioneer cells prior to the arrival of the primary motor axons, which included an increase in axonal branching and a delay in axonal growth of the CaP motor axon (Melancon et al., 1997). These defects are in part similar to the defects observed in N-cadherin mutants (increased axonal branching), and in neurons expressing ΔED N-cadherin cytoplasmic domain (stalled or delayed axonal growth), suggesting N-cadherin-mediated adhesion or signaling between motor axons and muscle pioneer cells contribute to regulate motor axons behavior. Alternatively, N-cadherin may cell-autonomously regulate axonal behavior at the horizontal myoseptum and during the innervation of the myotome. At the time the motor axons innervate the ventral myotome, fast muscle cell express M-cadherin (Cortes et al., 2003), which is not known to interact with N-cadherin. Thus, the increase in motor axon branching observed in N-cadherin depleted embryos may be due to the disruption cell-autonomous mechanisms regulated by N-cadherin.

One possible explanation for the effect of N-cadherin depletion on aberrant axonal growth is the regulation of cytoskeletal dynamics by N-cadherin. Cadherin adhesive interactions include the association with β-catenin and α-catenin, which participate in the organization of the actin cytoskeleton at sites of cell-cell contact (Ehrlich et al., 2002; Perez et al., 2008; Yap et al., 1997). Thus, removal of N-cadherin can affect regulatory mechanisms that control the cytoskeleton and interfere with growth cone behavior. For instance, overexpression of β-catenin in retinotectal projections causes an increase in axonal branching (Elul et al., 2003), while removal of αN-catenin results in abnormal filopodial-like extension of hippocampal dendritic spines (Togashi et al., 2002), indicating that interactions between N-cadherin and the actin cytoskeleton are necessary to restrain neurite growth. Furthermore, actin depolymerization in cultured hippocampal neurons leads to the loss of N-cadherin from synaptic sites and promotes formation of filopodial-like processes (Zhang and Benson, 2001), suggesting that regulation of the actin cytoskeleton by N-cadherin binding controls the shape and mobility of neuronal processes. In addition to the regulation of the cytoskeleton via the interaction with catenins, cadherin homotypic binding regulates Rho GTPases activity (Braga et al., 1997; Kovacs et al., 2002; Nakagawa et al., 2001; Noren et al., 2001), which controls cytoskeletal dynamics and axonal growth (Hall and Lalli, 2010), suggesting that disruption of N-cadherin activity may interfere with regulation of the cytoskeleton upstream of Rho GTPases.

Similar to the effect of N-cadherin depletion on primary motor axons growth, mosaic expression of dominant-interfering ΔED N-cadherin cytoplasmic domain in motor neurons did not affect axonal outgrowth. However, in contrast to the removal of N-cadherin from all cells, axon migration at the choice point was impaired by the expression of the ΔED cytoplasmic domain, suggesting that N-cadherin cell-autonomously regulate axonal behavior. ΔED N-cadherin cytoplasmic domain reduces cadherin-mediated adhesion and signaling by competing for cadherin cytosolic partners (Dufour et al., 1994; Fujimori and Takeichi, 1993; Katz et al., 1998; Kintner, 1992; Togashi et al., 2002). In addition, ΔED N-cadherin cytoplasmic domain may promote ectopic localization of cadherin binding proteins at sites in which their interactions with cadherin is normally regulated by cadherin homotypic binding. For instance, p120-catenin regulates cytoskeletal dynamics via its effects on Rho GTPases, and this activity is dependent on whether p120-catenin is bound to cadherins (Anastasiadis, 2007; Anastasiadis et al., 2000; Elia et al., 2006; Wildenberg et al.,

2006). Thus, depletion of catenins from the cytosol or abnormal accumulation of catenins at the cell membrane may affect N-cadherin-mediated signaling mechanisms and have downstream effects on cytoskeletal dynamics that interfere with the regulation of motor axon growth.

It is also possible that expression of ΔED N-cadherin cytoplasmic domain interferes with the function of other type I or type II cadherins that might be expressed by motor neurons. Although the repertoire of cadherins expressed by zebrafish motor neurons has not been determined, different motor neuronal pools in the chick spinal cord express different cadherins, which participate in the establishment of neuronal circuits (Price et al., 2002). The catenin binding sites of cadherin cytoplasmic domains are highly conserved among type I and type II cadherins (Nollet et al., 2000), and therefore, expression of ΔED N-cadherin cytoplasmic domain used in this study would also affect the adhesive and/or signaling activities of other cadherins that may contribute to axonal growth.

Finally, analysis of the role of N-cadherin on axonal growth during *Drosophila* development showed that loss DN-cadherin did not affect axonal elongation of pioneer neurons; however, axonal innervation patterns became distorted when neurons invaded mesodermally derived tissues (Iwai et al., 1997). DN-cadherin also regulates axonal growth at specific choice points during formation of the visual and olfactory system (Hummel and Zipursky, 2004; Lee et al., 2001). However, DN-cadherin does not play an instructive role in neuronal target selection in olfactory projection neurons, but rather, a role in regulating dendritic and axonal arborization and stabilization (Iwai et al., 1997; Zhu and Luo, 2004). Thus, similar to the findings in DN-cadherin mutants, defective axonal growth in zebrafish motor neurons does not appear to be due to the loss of axon guidance, suggesting that N-cadherin regulates signaling mechanisms that affect cytoskeletal dynamics which in turn influence axon growth.

Acknowledgments

This work was in part supported by NIH grants P20 RR016475, P20 RR024214, and NICDH HD02528.

I thank X. Zhao for her assistance in maintaining the zebrafish colony, embryo injection, and immunostaining; T. A. Zelenchuk for his assistance in the construction and preparation of expression vectors; and C. S. Theisen, for the generation of the plasmid driving Gal4-VP16 under the *mnx1* promoter. I also thank C-B. Chien from the University of Utah for providing the Tol2 kit plasmids, J. D. Jontes from Ohio State University for providing the plasmid carrying zebrafish N-cadherin cDNA, Qin Liu from the University of Akron for providing the anti-zebrafish N-cadherin rabbit polyclonal antibody, D. Meyer from the University of Freiburg for providing a plasmid carrying the *mnx1* promoter, and M. Granato from the University of Pennsylvania for providing a plasmid carrying EGFP under the *mnx1* promoter and for his critical reading of the manuscript.

Literature Cited

Akins MR, Benson DL, Greer CA. Cadherin expression in the developing mouse olfactory system. J Comp Neurol. 2007; 501(4):483–497. [PubMed: 17278136]

Amsterdam A, Burgess S, Golling G, Chen W, Sun Z, Townsend K, Farrington S, Haldi M, Hopkins N. A large-scale insertional mutagenesis screen in zebrafish. Genes Dev. 1999; 13(20):2713–2724. [PubMed: 10541557]

Amsterdam A, Hopkins N. Retrovirus-mediated insertional mutagenesis in zebrafish. Methods Cell Biol. 1999; 60:87–98. [PubMed: 9891332]

Amsterdam A, Nissen RM, Sun Z, Swindell EC, Farrington S, Hopkins N. Identification of 315 genes essential for early zebrafish development. Proc Natl Acad Sci U S A. 2004; 101(35):12792–12797. [PubMed: 15256591]

Anastasiadis PZ. p120-ctn: A nexus for contextual signaling via Rho GTPases. Biochim Biophys Acta. 2007; 1773(1):34–46. [PubMed: 17028013]

Anastasiadis PZ, Moon SY, Thoreson MA, Mariner DJ, Crawford HC, Zheng Y, Reynolds AB. Inhibition of RhoA by p120 catenin. Nat Cell Biol. 2000; 2(9):637–644. [PubMed: 10980705]

Arber S, Han B, Mendelsohn M, Smith M, Jessell TM, Sockanathan S. Requirement for the homeobox gene Hb9 in the consolidation of motor neuron identity. Neuron. 1999; 23(4):659–674. [PubMed: 10482234]

Birely J, Schneider VA, Santana E, Dosch R, Wagner DS, Mullins MC, Granato M. Genetic screens for genes controlling motor nerve-muscle development and interactions. Dev Biol. 2005; 280(1): 162–176. [PubMed: 15766756]

Bitzur S, Kam Z, Geiger B. Structure and distribution of N-cadherin in developing zebrafish embryos: morphogenetic effects of ectopic over-expression. Dev Dyn. 1994; 201(2):121–136. [PubMed: 7873785]

Bixby JL, Zhang R. Purified N-cadherin is a potent substrate for the rapid induction of neurite outgrowth. J Cell Biol. 1990; 110(4):1253–1260. [PubMed: 2324197]

Bozdagi O, Valcin M, Poskanzer K, Tanaka H, Benson DL. Temporally distinct demands for classic cadherins in synapse formation and maturation. Mol Cell Neurosci. 2004; 27(4):509–521. [PubMed: 15555928]

Braga VM, Machesky LM, Hall A, Hotchin NA. The small GTPases Rho and Rac are required for the establishment of cadherin-dependent cell-cell contacts. J Cell Biol. 1997; 137(6):1421–1431. [PubMed: 9182672]

Brand AH, Perrimon N. Targeted gene expression as a means of altering cell fates and generating dominant phenotypes. Development. 1993; 118(2):401–415. [PubMed: 8223268]

Buckley K, Kelly RB. Identification of a transmembrane glycoprotein specific for secretory vesicles of neural and endocrine cells. J Cell Biol. 1985; 100(4):1284–1294. [PubMed: 2579958]

Cortes F, Daggett D, Bryson-Richardson RJ, Neyt C, Maule J, Gautier P, Hollway GE, Keenan D, Currie PD. Cadherin-mediated differential cell adhesion controls slow muscle cell migration in the developing zebrafish myotome. Dev Cell. 2003; 5(6):865–876. [PubMed: 14667409]

Davison JM, Akitake CM, Goll MG, Rhee JM, Gosse N, Baier H, Halpern ME, Leach SD, Parsons MJ. Transactivation from Gal4-VP16 transgenic insertions for tissue-specific cell labeling and ablation in zebrafish. Dev Biol. 2007; 304(2):811–824. [PubMed: 17335798]

Desai CJ, Gindhart JG Jr, Goldstein LS, Zinn K. Receptor tyrosine phosphatases are required for motor axon guidance in the Drosophila embryo. Cell. 1996; 84(4):599–609. [PubMed: 8598046]

Devoto SH, Melancon E, Eisen JS, Westerfield M. Identification of separate slow and fast muscle precursor cells in vivo, prior to somite formation. Development. 1996; 122(11):3371–3380. [PubMed: 8951054]

Dufour S, Saint-Jeannet JP, Broders F, Wedlich D, Thiery JP. Differential perturbations in the morphogenesis of anterior structures induced by overexpression of truncated XB- and N-cadherins in Xenopus embryos. J Cell Biol. 1994; 127(2):521–535. [PubMed: 7929592]

Ehrlich JS, Hansen MD, Nelson WJ. Spatio-temporal regulation of Rac1 localization and lamellipodia dynamics during epithelial cell-cell adhesion. Dev Cell. 2002; 3(2):259–270. [PubMed: 12194856]

Eisen JS, Myers PZ, Westerfield M. Pathway selection by growth cones of identified motoneurones in live zebra fish embryos. Nature. 1986; 320(6059):269–271. [PubMed: 3960108]

Eisen JS, Pike SH, Romancier B. An identified motoneuron with variable fates in embryonic zebrafish. J Neurosci. 1990; 10(1):34–43. [PubMed: 2299397]

Elia LP, Yamamoto M, Zang K, Reichardt LF. p120 catenin regulates dendritic spine and synapse development through Rho-family GTPases and cadherins. Neuron. 2006; 51(1):43–56. [PubMed: 16815331]

Elul TM, Kimes NE, Kohwi M, Reichardt LF. N- and C-terminal domains of beta-catenin, respectively, are required to initiate and shape axon arbors of retinal ganglion cells in vivo. J Neurosci. 2003; 23(16):6567–6575. [PubMed: 12878698]

Fambrough D, Goodman CS. The Drosophila beaten path gene encodes a novel secreted protein that regulates defasciculation at motor axon choice points. Cell. 1996; 87(6):1049–1058. [PubMed: 8978609]

Felsenfeld AL, Curry M, Kimmel CB. The fub-1 mutation blocks initial myofibril formation in zebrafish muscle pioneer cells. Dev Biol. 1991; 148(1):23–30. [PubMed: 1936560]

Flanagan-Steet H, Fox MA, Meyer D, Sanes JR. Neuromuscular synapses can form in vivo by incorporation of initially aneural postsynaptic specializations. Development. 2005; 132(20):4471–4481. [PubMed: 16162647]

Fox MA, Sanes JR. Synaptotagmin I and II are present in distinct subsets of central synapses. J Comp Neurol. 2007; 503(2):280–296. [PubMed: 17492637]

Fujimori T, Takeichi M. Disruption of epithelial cell-cell adhesion by exogenous expression of a mutated nonfunctional N-cadherin. Mol Biol Cell. 1993; 4(1):37–47. [PubMed: 8443408]

Goodman CS, Shatz CJ. Developmental mechanisms that generate precise patterns of neuronal connectivity. Cell. 1993; 72(Suppl):77–98. [PubMed: 8428376]

Gumbiner BM. Regulation of cadherin-mediated adhesion in morphogenesis. Nat Rev Mol Cell Biol. 2005; 6(8):622–634. [PubMed: 16025097]

Hall A, Lalli G. Rho and Ras GTPases in axon growth, guidance, and branching. Cold Spring Harb Perspect Biol. 2010; 2(2):a001818. [PubMed: 20182621]

Hatta K, Takagi S, Fujisawa H, Takeichi M. Spatial and temporal expression pattern of N-cadherin cell adhesion molecules correlated with morphogenetic processes of chicken embryos. Dev Biol. 1987; 120(1):215–227. [PubMed: 3817290]

Holmes AL, Heilig JS. Fasciclin II and Beaten path modulate intercellular adhesion in Drosophila larval visual organ development. Development. 1999; 126(2):261–272. [PubMed: 9847240]

Hummel T, Zipursky SL. Afferent induction of olfactory glomeruli requires N-cadherin. Neuron. 2004; 42(1):77–88. [PubMed: 15066266]

Iwai Y, Usui T, Hirano S, Steward R, Takeichi M, Uemura T. Axon patterning requires DN-cadherin, a novel neuronal adhesion receptor, in the Drosophila embryonic CNS. Neuron. 1997; 19(1):77–89. [PubMed: 9247265]

Jiang YJ, Brand M, Heisenberg CP, Beuchle D, Furutani-Seiki M, Kelsh RN, Warga RM, Granato M, Haffter P, Hammerschmidt M, Kane DA, Mullins MC, Odenthal J, van Eeden FJ, Nusslein-Volhard C. Mutations affecting neurogenesis and brain morphology in the zebrafish, Danio rerio. Development. 1996; 123:205–216. [PubMed: 9007241]

Jontes JD, Emond MR, Smith SJ. In vivo trafficking and targeting of N-cadherin to nascent presynaptic terminals. J Neurosci. 2004; 24(41):9027–9034. [PubMed: 15483121]

Kadowaki M, Nakamura S, Machon O, Krauss S, Radice GL, Takeichi M. N-cadherin mediates cortical organization in the mouse brain. Dev Biol. 2007; 304(1):22–33. [PubMed: 17222817]

Katsamba P, Carroll K, Ahlsen G, Bahna F, Vendome J, Posy S, Rajebhosale M, Price S, Jessell TM, Ben-Shaul A, Shapiro L, Honig BH. Linking molecular affinity and cellular specificity in cadherin-mediated adhesion. Proc Natl Acad Sci U S A. 2009

Katz BZ, Levenberg S, Yamada KM, Geiger B. Modulation of cell-cell adherens junctions by surface clustering of the N-cadherin cytoplasmic tail. Exp Cell Res. 1998; 243(2):415–424. [PubMed: 9743601]

Kawakami K, Koga A, Hori H, Shima A. Excision of the tol2 transposable element of the medaka fish, Oryzias latipes, in zebrafish, Danio rerio. Gene. 1998; 225(1–2):17–22. [PubMed: 9931412]

Kimmel CB, Ballard WW, Kimmel SR, Ullmann B, Schilling TF. Stages of embryonic development of the zebrafish. Dev Dyn. 1995; 203(3):253–310. [PubMed: 8589427]

Kintner C. Regulation of embryonic cell adhesion by the cadherin cytoplasmic domain. Cell. 1992; 69(2):225–236. [PubMed: 1568244]

Koster RW, Fraser SE. Tracing transgene expression in living zebrafish embryos. Dev Biol. 2001; 233(2):329–346. [PubMed: 11336499]

Kovacs EM, Goodwin M, Ali RG, Paterson AD, Yap AS. Cadherin-directed actin assembly: E-cadherin physically associates with the Arp2/3 complex to direct actin assembly in nascent adhesive contacts. Curr Biol. 2002; 12(5):379–382. [PubMed: 11882288]

Krueger NX, Van Vactor D, Wan HI, Gelbart WM, Goodman CS, Saito H. The transmembrane tyrosine phosphatase DLAR controls motor axon guidance in Drosophila. Cell. 1996; 84(4):611–622. [PubMed: 8598047]

Kwan KM, Fujimoto E, Grabher C, Mangum BD, Hardy ME, Campbell DS, Parant JM, Yost HJ, Kanki JP, Chien CB. The Tol2kit: a multisite gateway-based construction kit for Tol2 transposon transgenesis constructs. Dev Dyn. 2007; 236(11):3088–3099. [PubMed: 17937395]

Laemmli UK. Cleavage of structural proteins during the assembly of the head of bacteriophage T4. Nature. 1970; 227(5259):680–685. [PubMed: 5432063]

Lee CH, Herman T, Clandinin TR, Lee R, Zipursky SL. N-cadherin regulates target specificity in the Drosophila visual system. Neuron. 2001; 30(2):437–450. [PubMed: 11395005]

Lele Z, Folchert A, Concha M, Rauch GJ, Geisler R, Rosa F, Wilson SW, Hammerschmidt M, Bally-Cuif L. parachute/n-cadherin is required for morphogenesis and maintained integrity of the zebrafish neural tube. Development. 2002; 129(14):3281–3294. [PubMed: 12091300]

Leonard WJ, Depper JM, Crabtree GR, Rudikoff S, Pumphrey J, Robb RJ, Kronke M, Svetlik PB, Peffer NJ, Waldmann TA, et al. Molecular cloning and expression of cDNAs for the human interleukin-2 receptor. Nature. 1984; 311(5987):626–631. [PubMed: 6090948]

Liu DW, Westerfield M. The formation of terminal fields in the absence of competitive interactions among primary motoneurons in the zebrafish. J Neurosci. 1990; 10(12):3947–3959. [PubMed: 2269893]

Liu DW, Westerfield M. Clustering of muscle acetylcholine receptors requires motoneurons in live embryos, but not in cell culture. J Neurosci. 1992; 12(5):1859–1866. [PubMed: 1315852]

Liu Q, Babb SG, Novince ZM, Doedens AL, Marrs J, Raymond PA. Differential expression of cadherin-2 and cadherin-4 in the developing and adult zebrafish visual system. Vis Neurosci. 2001; 18(6):923–933. [PubMed: 12020083]

Matsunaga M, Hatta K, Nagafuchi A, Takeichi M. Guidance of optic nerve fibres by N-cadherin adhesion molecules. Nature. 1988; 334(6177):62–64. [PubMed: 3386742]

Matsunami H, Takeichi M. Fetal brain subdivisions defined by R- and E-cadherin expressions: evidence for the role of cadherin activity in region-specific, cell-cell adhesion. Dev Biol. 1995; 172(2):466–478. [PubMed: 8612964]

Melancon E, Liu DW, Westerfield M, Eisen JS. Pathfinding by identified zebrafish motoneurons in the absence of muscle pioneers. J Neurosci. 1997; 17(20):7796–7804. [PubMed: 9315900]

Myers PZ, Eisen JS, Westerfield M. Development and axonal outgrowth of identified motoneurons in the zebrafish. J Neurosci. 1986; 6(8):2278–2289. [PubMed: 3746410]

Nakagawa M, Fukata M, Yamaga M, Itoh N, Kaibuchi K. Recruitment and activation of Rac1 by the formation of E-cadherin-mediated cell-cell adhesion sites. J Cell Sci. 2001; 114(Pt 10):1829–1838. [PubMed: 11329369]

Neugebauer KM, Tomaselli KJ, Lilien J, Reichardt LF. N-cadherin, NCAM, and integrins promote retinal neurite outgrowth on astrocytes in vitro. Journal of Cell Biology. 1988; 107(3):1177–1187. [PubMed: 3262111]

Nollet F, Kools P, van Roy F. Phylogenetic analysis of the cadherin superfamily allows identification of six major subfamilies besides several solitary members. J Mol Biol. 2000; 299(3):551–572. [PubMed: 10835267]

Noren NK, Niessen CM, Gumbiner BM, Burridge K. Cadherin engagement regulates Rho family GTPases. J Biol Chem. 2001; 276(36):33305–33308. [PubMed: 11457821]

Panzer JA, Gibbs SM, Dosch R, Wagner D, Mullins MC, Granato M, Balice-Gordon RJ. Neuromuscular synaptogenesis in wild-type and mutant zebrafish. Dev Biol. 2005; 285(2):340–357. [PubMed: 16102744]

Panzer JA, Song Y, Balice-Gordon RJ. In vivo imaging of preferential motor axon outgrowth to and synaptogenesis at prepatterned acetylcholine receptor clusters in embryonic zebrafish skeletal muscle. J Neurosci. 2006; 26(3):934–947. [PubMed: 16421313]

Payne HR, Burden SM, Lemmon V. Modulation of growth cone morphology by substrate-bound adhesion molecules. Cell Motil Cytoskeleton. 1992; 21(1):65–73. [PubMed: 1540993]

Perez TD, Tamada M, Sheetz MP, Nelson WJ. Immediate-early signaling induced by E-cadherin engagement and adhesion. J Biol Chem. 2008; 283(8):5014–5022. [PubMed: 18089563]

Price SR, De Marco Garcia NV, Ranscht B, Jessell TM. Regulation of motor neuron pool sorting by differential expression of type II cadherins. Cell. 2002; 109(2):205–216. [PubMed: 12007407]

Redies C, Takeichi M. Cadherins in the developing central nervous system: an adhesive code for segmental and functional subdivisions. Dev Biol. 1996; 180(2):413–423. [PubMed: 8954714]

Riehl R, Johnson K, Bradley R, Grunwald GB, Cornel E, Lilienbaum A, Holt CE. Cadherin function is required for axon outgrowth in retinal ganglion cells in vivo. Neuron. 1996; 17(5):979–990. [PubMed: 8938129]

Sanes JR, Lichtman JW. Development of the vertebrate neuromuscular junction. Annu Rev Neurosci. 1999; 22:389–442. [PubMed: 10202544]

Scheer N, Campos-Ortega JA. Use of the Gal4-UAS technique for targeted gene expression in the zebrafish. Mech Dev. 1999; 80(2):153–158. [PubMed: 10072782]

Stockinger H, Valent P, Majdic O, Bettelheim P, Knapp W. Human blood basophils synthesize interleukin-2 binding sites. Blood. 1990; 75(9):1820–1826. [PubMed: 1691935]

Suster ML, Kikuta H, Urasaki A, Asakawa K, Kawakami K. Transgenesis in zebrafish with the tol2 transposon system. Methods Mol Biol. 2009; 561:41–63. [PubMed: 19504063]

Takeichi M. Cadherin cell adhesion receptors as a morphogenetic regulator. Science. 1991; 251(5000): 1451–1455. [PubMed: 2006419]

Takeichi M. The cadherin superfamily in neuronal connections and interactions. Nat Rev Neurosci. 2007; 8(1):11–20. [PubMed: 17133224]

Tanabe Y, William C, Jessell TM. Specification of motor neuron identity by the MNR2 homeodomain protein. Cell. 1998; 95(1):67–80. [PubMed: 9778248]

Tang J, Landmesser L, Rutishauser U. Polysialic acid influences specific pathfinding by avian motoneurons. Neuron. 1992; 8(6):1031–1044. [PubMed: 1319183]

Tepass U, Truong K, Godt D, Ikura M, Peifer M. Cadherins in embryonic and neural morphogenesis. Nat Rev Mol Cell Biol. 2000; 1(2):91–100. [PubMed: 11253370]

Togashi H, Abe K, Mizoguchi A, Takaoka K, Chisaka O, Takeichi M. Cadherin regulates dendritic spine morphogenesis. Neuron. 2002; 35(1):77–89. [PubMed: 12123610]

Trevarrow B, Marks DL, Kimmel CB. Organization of hindbrain segments in the zebrafish embryo. Neuron. 1990; 4(5):669–679. [PubMed: 2344406]

von der Hardt S, Bakkers J, Inbal A, Carvalho L, Solnica-Krezel L, Heisenberg CP, Hammerschmidt M. The Bmp gradient of the zebrafish gastrula guides migrating lateral cells by regulating cell-cell adhesion. Curr Biol. 2007; 17(6):475–487. [PubMed: 17331724]

Warga RM, Kane DA. A role for N-cadherin in mesodermal morphogenesis during gastrulation. Dev Biol. 2007; 310(2):211–225. [PubMed: 17826762]

Westerfield, M. The zebrafish book. A guide for the laboratory use of zebrafish (Danio rerio). Eugene, OR: University of Oregon Press; 2000.

Westerfield M, McMurray JV, Eisen JS. Identified motoneurons and their innervation of axial muscles in the zebrafish. J Neurosci. 1986; 6(8):2267–2277. [PubMed: 3746409]

Wildenberg GA, Dohn MR, Carnahan RH, Davis MA, Lobdell NA, Settleman J, Reynolds AB. p120-catenin and p190RhoGAP regulate cell-cell adhesion by coordinating antagonism between Rac and Rho. Cell. 2006; 127(5):1027–1039. [PubMed: 17129786]

Winberg ML, Noordermeer JN, Tamagnone L, Comoglio PM, Spriggs MK, Tessier-Lavigne M, Goodman CS. Plexin A is a neuronal semaphorin receptor that controls axon guidance. Cell. 1998; 95(7):903–916. [PubMed: 9875845]

Yap AS, Brieher WM, Gumbiner BM. Molecular and functional analysis of cadherin-based adherens junctions. Annu Rev Cell Dev Biol. 1997; 13:119–146. [PubMed: 9442870]

Yu HH, Araj HH, Ralls SA, Kolodkin AL. The transmembrane Semaphorin Sema I is required in Drosophila for embryonic motor and CNS axon guidance. Neuron. 1998; 20(2):207–220. [PubMed: 9491983]

Zhang J, Granato M. The zebrafish unplugged gene controls motor axon pathway selection. Development. 2000; 127(10):2099–2111. [PubMed: 10769234]

Zhang W, Benson DL. Stages of synapse development defined by dependence on F-actin. J Neurosci. 2001; 21(14):5169–5181. [PubMed: 11438592]

Zhu H, Luo L. Diverse functions of N-cadherin in dendritic and axonal terminal arborization of olfactory projection neurons. Neuron. 2004; 42(1):63–75. [PubMed: 15066265]

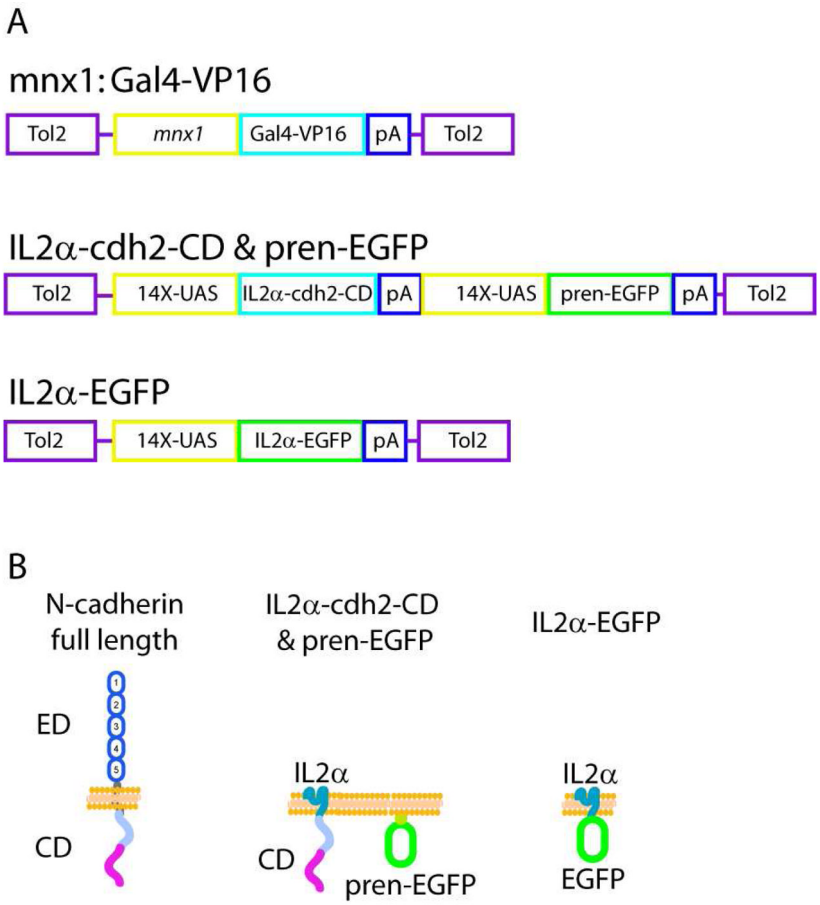

Figure 1.

A) Schematic representation of the plasmids used to generate a stable transgenic fish expressing Gal4-VP16 in motor neurons under the *mnx1* promoter, and the vectors used for expressing N-cadherin cytoplasmic domain fused to the IL2α subunit receptor (IL2α-cdh2-CD & pren-EGFP) and IL2α C-terminally fused to EGFP (IL2α-EGFP). B) Schematic representation of full length N-cadherin and domain-deleted constructs used as dominant-interfering proteins. ED, ectodomain; CD, cytoplasmic domain.

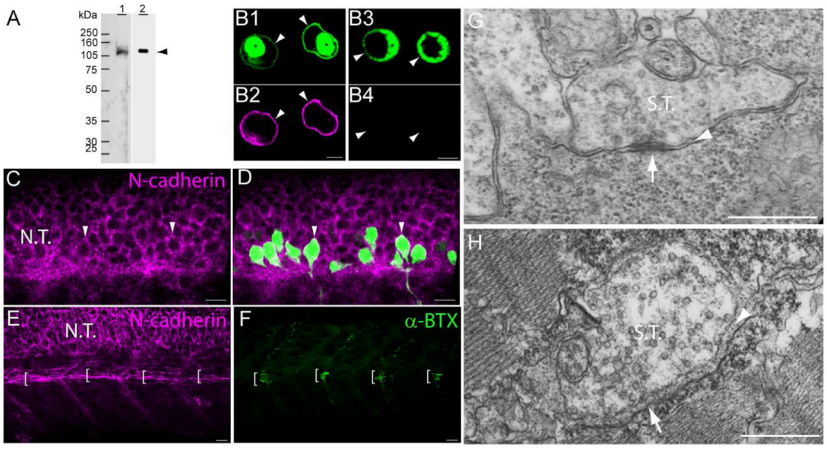

Figure 2.

N-cadherin expression in primary motor neurons and muscle pioneer cells. A) Western blot analysis of anti-N-cadherin antibodies (see Table 1). Zebrafish (72hpf) homogenates (40 μg of total protein/lane) were electrophoresed in a 10% SDS-polyacrylamide gel, electro-transferred to a PVDF membrane, and immunoblotted with a rabbit polyclonal anti-zebrafish N-cadherin (lane 1) and MNCD2 monoclonal anti-mouse N-cadherin (lane 2) antibodies. A single band of ~120 kDa was detected in lane 1 and lane 2 by the rabbit polyclonal and MNCD2 antibodies respectively (arrowhead). B) CHO cells were transfected with a plasmid expressing Gal4 under a CMV promoter and a plasmid carrying zebrafish N-cadherin and pren-EGFP under a 14X-UAS element (B1, B2), or a plasmid expressing pren-EGFP under a 14X-UAS (B3, B4). Cells were fixed and immunostained with anti-N-cadherin MNCD2 antibodies and anti-rat IgG Cy3-conjugated secondary antibodies. B1 and B2) confocal images of the same cells showing expression of EGFP (B1) and N-cadherin (B2). B3 and B4) confocal images of the same cells showing expression of EGFP (B3) while no N-cadherin labeling is detected (B4). Arrowheads point to the cell membrane and asterisks indicate the perinuclear region. C and D) Neural tube of 24 hpf *Tg(mnx1:GFP)* embryos immunostained with anti-N-cadherin MNCD2 antibodies and observed under confocal microscopy. Arrowheads point to primary motor neurons cell bodies labeled with EGFP and expressing N-cadherin on the cell surface. E and F) Wild type zebrafish embryos (24 hpf) double-labeled with anti-N-cadherin MNCD2 antibodies (E) and with α-bungarotoxin (α-BTX) conjugated with Alexa 488 to detect nicotinic acetylcholine receptors (F). Brackets indicate the muscle pioneer cells at the horizontal myoseptum expressing N-cadherin (E), and a distinct cluster of acetylcholine receptors (F). G) Electron micrograph of a neuromuscular junction at the horizontal myoseptum from a 24 hpf wild type zebrafish embryo. The arrowhead points to the synaptic cleft and the arrow to an active zone. H) Electron micrograph of a neuromuscular junction from a 120 hpf wild type zebrafish larvae. The arrowhead points to the synaptic cleft containing a characteristic basal lamina and the arrow points to an active zone determined by the presence synaptic vesicles fused to the presynaptic membrane. Scale bars in B, 5 μm; scale bar in C, D, E and F, 10 μm; scale bar in G and H, 0.5 μm; N.T., Neural Tube; S.T., Synaptic Terminal. Panels C to F, rostral is to the left and dorsal is to the top.

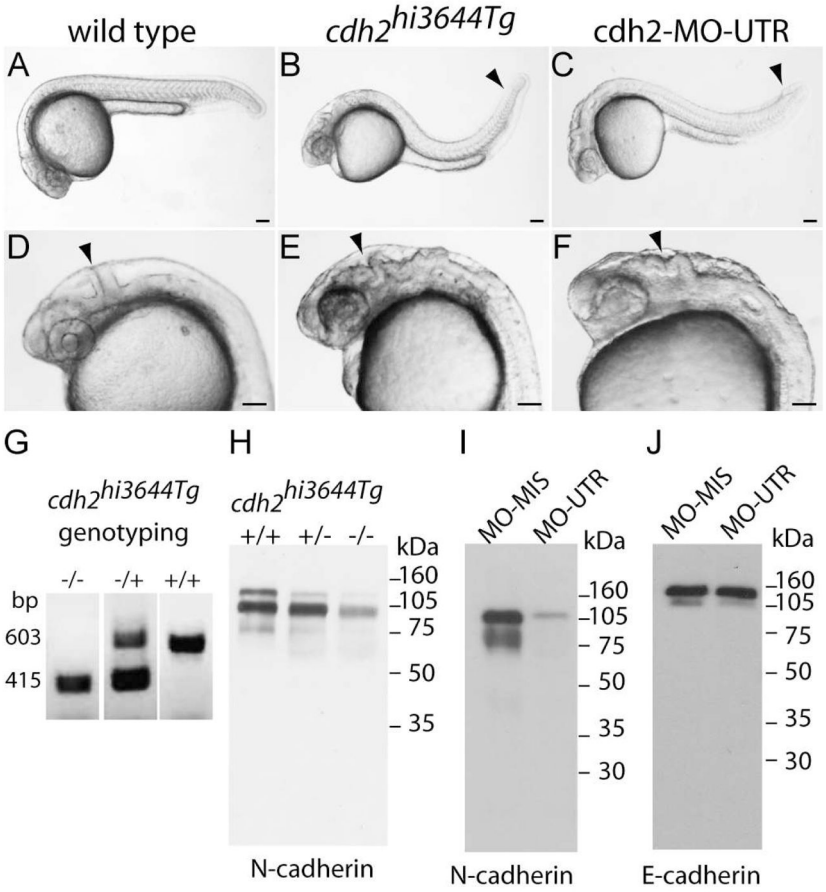

Figure 3.

Analysis of *cdh2*^{hi3644Tg} N-cadherin mutant zebrafish embryos. A, D) Photographs of 24 hpf wild type zebrafish embryos. The arrowhead in D points to the midbrain-hindbrain boundary. B, E) 24 hpf *cdh2*^{hi3644Tg} homozygote mutant embryos show defective tail (B, arrowhead) and disruption of the midbrain-hindbrain boundary (E, arrowhead). C and F) 24 hpf zebrafish embryos injected at the 1-cell stage with antisense N-cadherin morpholinos (cdh2-MO-UTR). Knock-down of N-cadherin expression causes defective tail morphogenesis (C, arrowhead) and loss of midbrain-hindbrain boundary (F, arrowhead). G) Genotyping of *cdh2*^{hi3644Tg} embryos: +/+) wild type, forward and reverse primers anneal to N-cadherin (603 bp); (−/−) homozygotes, forward primer anneals to the viral sequence and reverse primer anneals to N-cadherin sequence (415 bp); (−/+) heterozygotes, both bands are detected. H) Immunoblot analysis of N-cadherin expression in tissue homogenates from 24 hpf embryos obtained from a cross of *cdh2*^{hi3644Tg} heterozygote mutants. Embryos were genotyped and pooled as wild type (+/+), heterozygote (+/−), and homozygote (−/−) and homogenates electrophoresed in a 10% SDS-polyacrylamide gel, transferred to a PVDF membrane, immunoblotted with MNCD2 antibodies, and detected by chemiluminescence. MNCD2 antibodies detected two bands of ~105 kDa and ~120 kDa. Densitometric analysis was used to quantify the relative amount of N-cadherin in each sample, and expressed as percentage of wild type: (+/+) wild type 100%, (+/−) heterozygote 64%, and (−/−) homozygote 22%. I) Immunoblot analysis with MNCD2 antibodies of N-cadherin expression in 96 hpf wild type zebrafish larvae injected at the 1-cell stage with antisense morpholinos against N-cadherin UTR (MO-UTR). Embryos injected with an N-cadherin antisense mismatched morpholino (MO-MIS) were used as control. MNCD2 detected two

bands of ~105 kDa and ~120 kDa. J) Western blot of the same samples electrophoresed in (I) and immunoblotted with anti-E-cadherin antibodies revealed two bands of ~120 kDa and ~140k Da. E-cadherin protein expression levels were not affected by injection with N-cadherin antisense morpholinos. Scale bar in A to F, 0.1 mm.

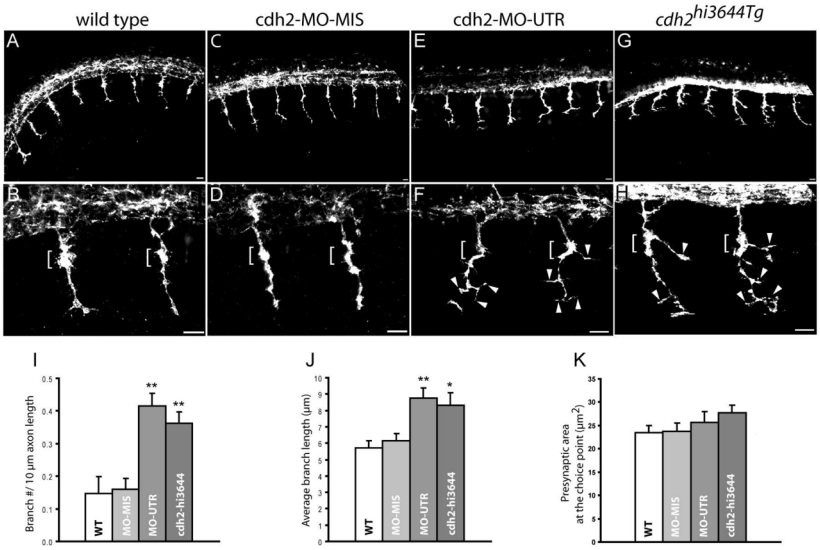

Figure 4.

Loss of N-cadherin expression affects primary motor axons branching. A – H) Lateral views of 24 hpf zebrafish embryos immunostained with SV2 and znp1 antibodies, and observed under confocal microscopy. A, B) Primary motor axons in wild type embryos exited the spinal cord and grew ventrally towards the horizontal myoseptum. The axons are enlarged at the area of contact with the muscle pioneer cells (brackets in B and D). C, D) Zebrafish embryos injected with N-cadherin antisense mismatched morpholinos (cdh2-MO-MIS) display axonal morphologies similar to wild type embryos. E, F) Embryos injected with antisense N-cadherin morpholino (cdh2-MO-UTR) reached the horizontal myoseptum but grew aberrant branches at the choice point (brackets) and in the ventral myotome (arrowheads). An axon branch is an extension of the axon from the center of the axon shaft >3 μm long. G, H) In *cdh2*^{hi3644Tg} homozygote embryos, motor axons formed aberrant branches at the choice point (brackets) and ventral to the horizontal myoseptum (arrowheads). I) Analysis of the number of branches per 10 μm of axon expressed as mean ± SE (wild type n = 27; cdh2-MO-MIS n = 29; cdh2-MO-UTR n = 26; *cdh2*^{hi3644Tg} n = 26 (n, number of axons analyzed). H) Analysis of the average length of the branches expressed as mean ± SE (wild type n = 21; cdh2-MO-MIS n = 27; cdh2-MO-UTR n = 51; *cdh2*^{hi3644Tg} n = 47 (n, number of branches examined)). Analysis of the presynaptic surface area at the choice point expressed as mean ± SE (wild type n = 48; cdh2-MO-MIS n = 44; cdh2-MO-UTR n = 31; *cdh2*^{hi3644Tg} n = 29 (n, number of axons examined)). T-test comparison of mutant and morpholino injected embryos versus wild type samples, ** $p < 0.005$, * $p < 0.05$. Scale bars, 10 μm. WT; wild type. Rostral is to the left and dorsal is to the top.

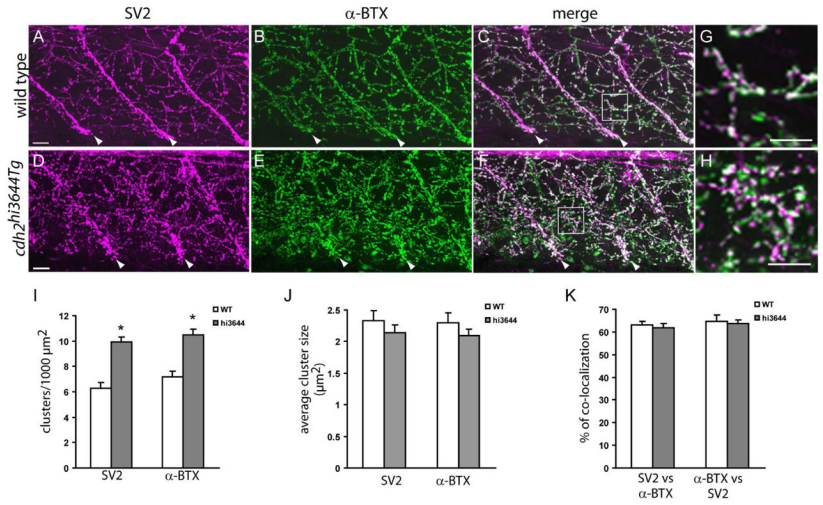

Figure 5.

N-cadherin *cdh2*^{hi3644Tg} mutants form higher number of neuromuscular junctions. Confocal images obtained from 120 hpf wild type (A – C) and *cdh2*^{hi3644Tg} (D – F) larvae double-labeled SV2 antibodies (A, D) and anti-mouse IgG Cy3 conjugated secondary antibody, and with α-bungarotoxin (α-BTX) conjugated to Alexa 488 (B, E). Approximately 30-μm thick stacks of confocal images obtained at 1 μm intervals were projected to a single plane. C, F) Merged images from A – B and D – E respectively. Arrowheads point to the somitic myoseptum. G, H) High-magnification images of the squares drawn in C and F respectively. I – K) Analysis of the number (I) and size (J) of SV2 and α-BTX clusters, and of the percentage of co-localization between pre and postsynaptic markers (K). Three confocal sections at the central region of the myotome were rendered to a single plane and used for the quantification of the SV2 and α-BTX clusters. Open bars, wild type (WT, n = 16) and gray bars *cdh2*^{hi3644Tg} (hi3644, n=27) (n, number of somitic hemisegments analyzed). Asterisks in I indicate a Student's t test p-value < 0.005. Scale bar in A and D, 10 μm; scale bar in G and H, 10 μm. Rostral is to the left and dorsal is to the top.

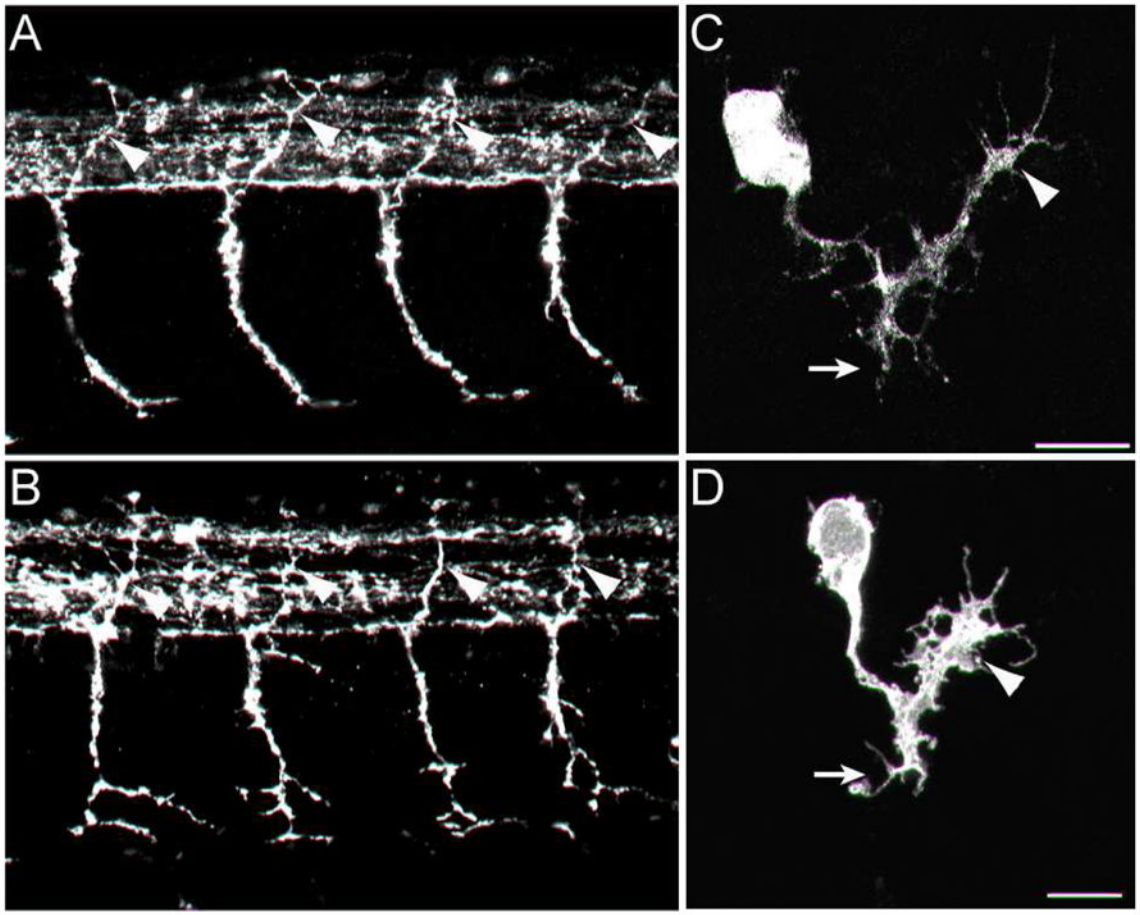

Figure 6.

MiP motor axon targeting is unaffected in N-cadherin mutant embryos. Wild type (A) and *cdh2*^{hi3644Tg} mutant embryos (B) were fixed at 27 hpf, immunolabeled with znp1 antibodies, and observed under confocal microscopy. Arrowheads point to the presumptive MiP axon in the dorsal myotome. The axons appear to have followed a distorted pattern of migration. C, D) Single MiP motor neurons labeled by mosaic expression of pren-EGFP using a mix of a plasmid expressing Gal4 under the *mnx1* promoter and a plasmid expressing pren-EGFP under a 14X-UAS element. In all cases, the motor axons reached the horizontal myoseptum and extended a dorsal branch. Scale bars, 10 μm; wild type, n = 6; *cdh2*^{hi364Tg} mutant, n = 6. Rostral is to the left and dorsal is to the top.

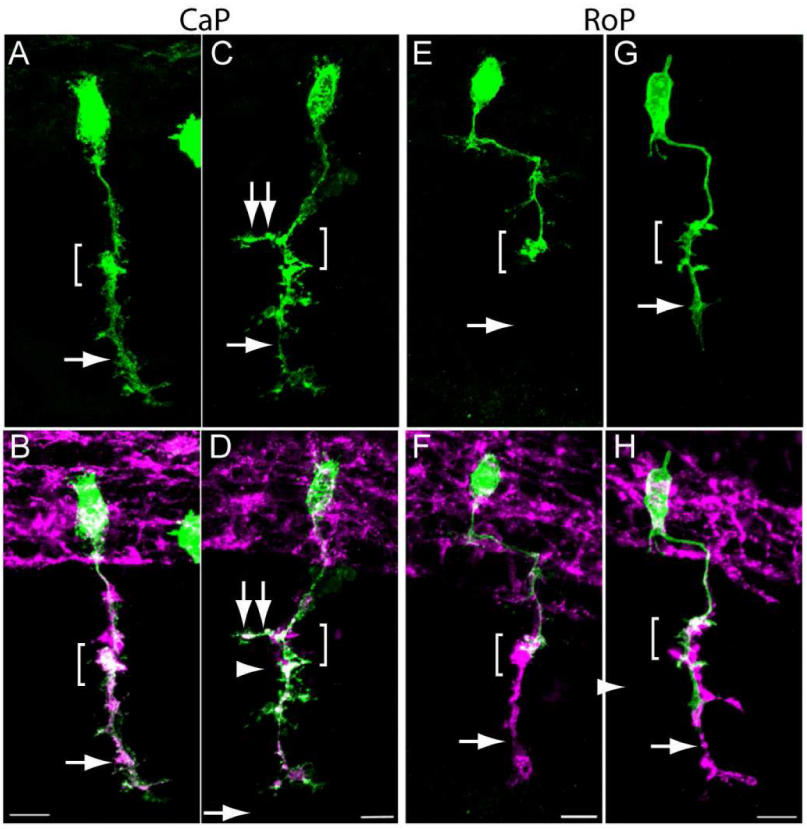

Figure 7.

CaP and RoP motor axons grow abnormal branches in N-cadherin mutant embryos. Wild type and *cdh2*^{hi3644Tg} embryos were injected at the 1-cell stage with a mix of two plasmids expressing Gal4 under the *mnx1* promoter and pren-EGFP under a 14X-UAS element, fixed at 24 hpf, immunolabeled with SV2 and znp1 antibodies, and observed under confocal microscopy. Images in A, C, E, and G show pren-EGFP labeling while images B, D, F, and H show pren-EGFP (green) merged with SV2 and znp1 antibody labeling. A, B) Wild type CaP motor neuron shows the characteristic morphology with an axon extending from the spinal cord, along the common pathway and into the myotome (arrow) ventral to the choice point (bracket). C, D) CaP motor neuron from a *cdh2*^{hi3644Tg} embryo. The bracket indicates the choice point, the arrow points to the axon in the ventral myotome, and the double arrows point to an aberrant branch extending in the rostrocaudal axis. E, F) Wild type RoP motor axon shows the characteristic caudal migration before turning ventrally into the myotome. The bracket indicates the choice point where the RoP axon normally stalled. The SV2 and znp1 labeling ventral to the choice point corresponds to the CaP motor axon. G, H) RoP motor neuron from a *cdh2*^{hi3644Tg} mutant embryo. The bracket indicates the choice point and the arrow points to aberrant growth of the axon into the ventral myotome together with the CaP motor axon. Scale bars, 10 μm. Rostral is to the left and dorsal is to the top.

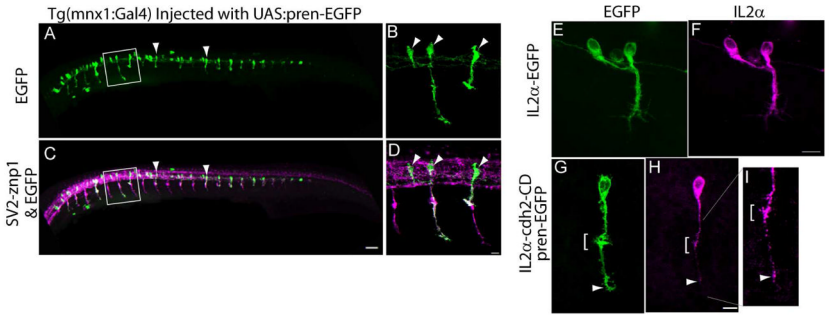

Figure 8.

A – D) *Tg(mnx1:Gal4-VP16)* embryos were injected at the 1-cell stage with a plasmid encoding pren-EGFP under a 14X-UAS element, fixed at 24 hpf, and immunostained with SV2 and znp1 antibodies. Arrowheads point to primary motor neurons expressing EGFP. B, D) higher magnification images of the squares drawn in A and C respectively. Arrowheads point to primary motor neurons somas. E – I) *Tg(mnx1:Gal4-VP16)* embryos were injected at the 1-cell stage with the 14X-UAS-IL2α-EGFP plasmid (E, F) or with 14X-UAS-IL2α-CD & pren-EGFP plasmid (G – I). Embryos were fixed at 24 hpf, and immunostained with anti-IL2α antibodies (F, H, and I). IL2α-EGFP is evenly distributed throughout the motor neuron (E, F). Pren-EGFP labels the entire cell body and axon (G) while IL2α-CD is detected as discrete puncta through out the cell (H, arrowheads). I) Higher magnification of the axon shown in (G) indicating IL2α-CD puncta accumulated at the choice point (bracket) and at the distal tip of the axon. Scale bar in C, 50 μm; Scale bar in D, 10 μm; Scale bar in F and H, 10 μm. Dorsal is to the top and rostral is to the left.

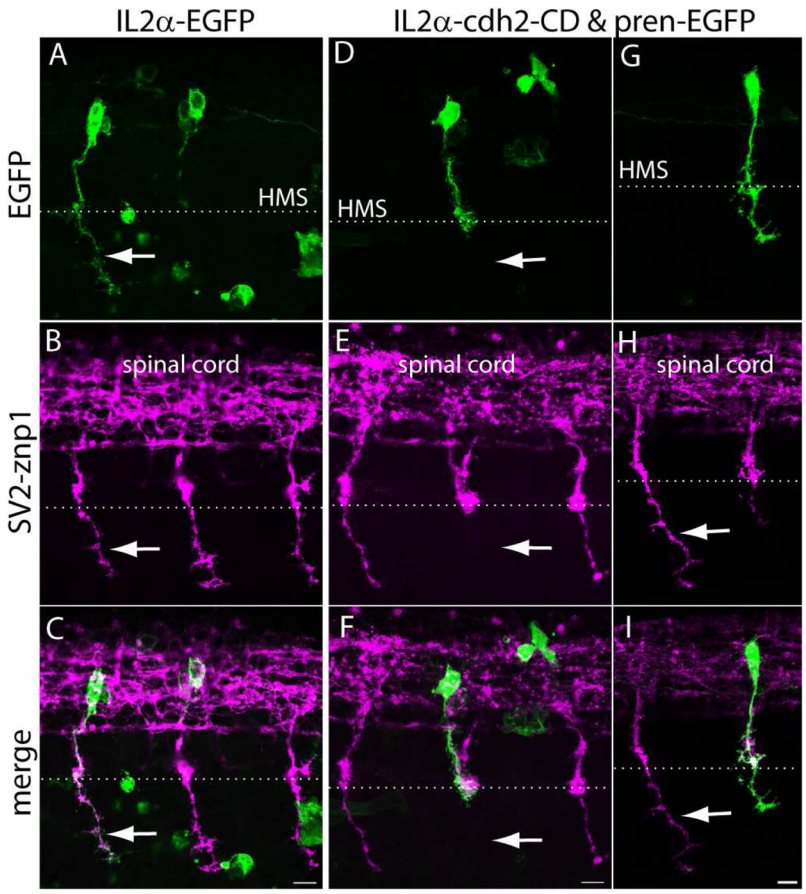

Figure 9.

Expression of N-cadherin dominant-interfering cytoplasmic domain perturbs CaP motor axon growth at the horizontal myoseptum. A – I) *Tg(mnx1:Gal4-VP16)* embryos were injected at the 1-cell stage with IL2α-EGFP (A – C) or with IL2α-cdh2-CD & pren-EGFP (D – I) plasmids. Embryos were fixed at 24 hpf, immunostained with SV2 and znp1 and observed under confocal microscopy. A – C) The arrow points to the CaP axon extending ventral to the horizontal myoseptum (HMS) indicated with a dashed line. The IL2α-EGFP labeled axon has a normal morphology as compared with the untransfected neighboring axons labeled with SV2 and znp1. D – F) A motor axon expressing IL2α-cdh2-CD grew through the common pathway but stalled at the horizontal myoseptum. The arrow points to the absence of SV2 and znp1 labeled CaP axon ventral to the choice point while neighboring untransfected axons grew normally. G – I) A CaP motor neuron expressing IL2α-cdh2-CD and pren-EGFP in which the axon extended ventrally to the horizontal myoseptum but shows a shorter migration distance as compared with an untransfected SV2 and znp1 labeled axon (arrow). Scale bar in C, F, and I, 10 μm. Dorsal is to the top and rostral is to the left.

Table 1

Antibodies

Name	Immunogen	Source & Catalog No	Species	Isotype
Znp1	Zebrafish synaptotagmin II	DSHB	mouse	monoclonal IgG2a
SV2	Elasmobranch synaptic vesicles	DSHB	mouse	monoclonal IgG1
Cdh2	Zebrafish N-cadherin extracellular domain amino acid residues 1 to 107	Gift from Q. Liu	rabbit	polyclonal IgG
MNCD2	Mouse N-cadherin extracellular domain amino acids residues 308 to 597	DSHB	rat	monoclonal IgG
36/E-cadherin	Human E-cadherin cytoplasmic domain amino acid residues 735 to 883	BD Transduction Labs 610181	mouse	monoclonal IgG2aK
CD25-3G10	Human interleukine-2α subunit	Caltag MHCD2500	mouse	monoclonal IgG1

Table 2

Analysis of motor axon defects in 24 hpf wild type and N-cadherin depleted embryos

	Hemisegments with no motor axons exiting the spinal cord	Hemisegments with motor axons stalled at the choice point	Hemisegments with motor axons branching at the choice point	Hemisegments with motor axons with >2 branches after the choice point	Hemisegments with motor axons with wild type morphology
wild type	0% (0/65) *	3.1% (2/65)	6.2% (4/65)	4.6% (3/65)	89.2% (58/65)
cdh2-MO-MISS	0% (0/27)	3.7% (1/27)	0% (0/27)	0% (0/27)	96.3% (26/27)
cdh2-MO-UTR	0% (0/68)	5.9% (4/68)	33.8% (23/68)	55.9% (38/68)	36.8% (25/68)
cdh2^{hi3644Tg}	5.2% (3/58)	0% (0/58)	44.8% (26/58)	58.6% (34/58)	24.1% (14/58)

* number of somitic hemisegments analyzed.

Number of embryos examined: wild type, n = 7; cdh2-MO-MIS, n = 4; cdh2-MO-UTR, n = 12; and *cdh2*^{hi3644Tg}, n = 9.

Table 3

Analysis of MiP motor axons

	Somitic segments with a dorsal axonal projection	Axons in the dorsal myotome with wild type phenotype
wild type	100% (66/66)	97.0% (64/66)
cdh2^{hi3644Tg}	100% (76/76)	69.7% (53/76)

Table 4

Analysis of CaP and RoP motor axons

	CaP axons stalled at the choice point	CaP axons branched at the choice point	CaP axons with wild type projection	RoP axons stalled at the choice point	RoP axons branched at the choice point	RoP axons extending ventral to the choice point	RoP axons with wild type projection
wild type	0% (0/18) *	5.6% (1/18)	94.4% (17/18)	100% (9/9)	0% (0/9)	0% (0/9)	100% (9/9)
cdh2^{hi3644Tg}	0% (0/11)	27.3% (3/11)	9.1% (1/11)	77.8% (7/9)	33.3% (3/9)	22.2% (2/9)	44.4% (4/9)

* number of cells analyzed.

An axonal branch was considered an extension from the main axon >3 μm long from the center of the axon shaft.

Table 5

Effect of a dominant-interfering N-cadherin cytoplasmic domain on CaP motor axon growth

	CaP axons that reached the choice point	CaP axons that stalled at the choice point	CaP axons with abnormal morphology ventral to choice point	CaP axons with wild type projections
IL2α-EGFP	100% (17/17)*	0% (0/17)	11.8% (2/17)	88.2% (15/17)
IL2α-N-cadherin CD	100% (27/27)	25.9% (7/27)	25.9% (7/27)	48.1% (13/27)

*number of cells analyzed